

**University of Alberta**

**Muscle Spindle Ia afferents: cat models applied to human data**

by

Puja Malik 

A thesis submitted to the Faculty of Graduate Studies and Research  
in partial fulfillment of the requirements for the degree of

**Master of Science**

**Department of Biomedical Engineering**

**Edmonton, Alberta  
Fall 2006**



Library and  
Archives Canada

Bibliothèque et  
Archives Canada

Published Heritage  
Branch

Direction du  
Patrimoine de l'édition

395 Wellington Street  
Ottawa ON K1A 0N4  
Canada

395, rue Wellington  
Ottawa ON K1A 0N4  
Canada

*Your file* *Votre référence*  
*ISBN: 978-0-494-22314-7*  
*Our file* *Notre référence*  
*ISBN: 978-0-494-22314-7*

**NOTICE:**

The author has granted a non-exclusive license allowing Library and Archives Canada to reproduce, publish, archive, preserve, conserve, communicate to the public by telecommunication or on the Internet, loan, distribute and sell theses worldwide, for commercial or non-commercial purposes, in microform, paper, electronic and/or any other formats.

The author retains copyright ownership and moral rights in this thesis. Neither the thesis nor substantial extracts from it may be printed or otherwise reproduced without the author's permission.

**AVIS:**

L'auteur a accordé une licence non exclusive permettant à la Bibliothèque et Archives Canada de reproduire, publier, archiver, sauvegarder, conserver, transmettre au public par télécommunication ou par l'Internet, prêter, distribuer et vendre des thèses partout dans le monde, à des fins commerciales ou autres, sur support microforme, papier, électronique et/ou autres formats.

L'auteur conserve la propriété du droit d'auteur et des droits moraux qui protègent cette thèse. Ni la thèse ni des extraits substantiels de celle-ci ne doivent être imprimés ou autrement reproduits sans son autorisation.

---

In compliance with the Canadian Privacy Act some supporting forms may have been removed from this thesis.

Conformément à la loi canadienne sur la protection de la vie privée, quelques formulaires secondaires ont été enlevés de cette thèse.

While these forms may be included in the document page count, their removal does not represent any loss of content from the thesis.

Bien que ces formulaires aient inclus dans la pagination, il n'y aura aucun contenu manquant.

  
**Canada**

## **Abstract**

Muscle spindle primary afferents have been well characterized in cats. Many models have been introduced over the past four decades that attempt to quantitatively describe their firing rate response. Up until now, these models have only been tested against cat data. The goal of this study was to determine whether any of the six well-known cat muscle spindle primary afferent models can generalize to predict data in response to *human* movement. Data from eight human afferents was previously recorded while subjects performed a centre-out task. These recorded firing rates were compared to the predictions of the models in response to the same movement. It was found that three of the six models predict human primary afferent responses quite well, and these are the same three models that are the best predictors of cat data. From these results it can be inferred that cat and human primary afferents share similar response properties.

## **Acknowledgements**

I would like to gratefully thank my supervisor Dr. Kelvin E. Jones for his guidance, support, feedback and passion throughout this work. Sincere gratitude goes to the Whitaker Foundation for supporting this project, and CIHR for a student stipend. I would also like to acknowledge the other members of my thesis committee, Dr. Gorassini and Dr. Stein for their input and support at annual thesis meetings. I am indebted to Lora Major for her insightful discussions and help creating many of the figures in this thesis. I would also like to extend my gratitude to Yi Mao for his moral support.

## Table of Contents

---

<b>CHAPTER 1. INTRODUCTION AND MOTIVATION.....</b>	<b>1</b>
<b>1.1 Big picture.....</b>	<b>1</b>
Basic science perspective.....	1
Clinical relevance.....	4
Unanswered research questions addressed in this thesis.....	6
<b>1.2 Primary methodological approach in the thesis .....</b>	<b>7</b>
Experimental Data .....	8
Modelling.....	8
Analysis .....	9
<b>1.3 Thesis organization .....</b>	<b>9</b>
<b>CHAPTER 2. BACKGROUND AND LITERATURE REVIEW .....</b>	<b>11</b>
<b>2.1 Proprioception.....</b>	<b>11</b>
A Sixth Sense.....	11
Types of Proprioceptors.....	13
<b>2.2 Muscle Spindles .....</b>	<b>14</b>
<b>Distribution.....</b>	<b>15</b>
<b>Morphology .....</b>	<b>16</b>
Shape and Size .....	16
Intrafusal fibres .....	16
Afferent Innervation.....	18

Efferent Innervation .....	19
<b>Response Properties</b> .....	<b>20</b>
Secondary afferent response.....	20
Primary afferent response.....	21
Influence of fusimotor system.....	22
<b>2.3 Computational Models</b> .....	<b>24</b>
<b>Examples of Modelling in Physiology</b> .....	<b>25</b>
<b>Muscle Spindle Models</b> .....	<b>26</b>
Spindle Model Simplifications and their Implications .....	27
<b>Comparison of the six models in cats</b> .....	<b>28</b>
<b>Six Firing Rate Models</b> .....	<b>29</b>
<i>Prochazka &amp; Gorassini 1</i> .....	29
<i>Prochazka &amp; Gorassini 2</i> .....	30
<i>Houk et al</i> .....	30
<i>Matthews &amp; Stein</i> .....	31
<i>Chen &amp; Poppele</i> .....	33
<i>Hasan</i> .....	34
<b>Using the Models in this Thesis</b> .....	<b>36</b>
<b>CHAPTER 3. METHODS</b> .....	<b>37</b>
<b>3.1 Overview</b> .....	<b>37</b>
<b>3.2 Human Experiments</b> .....	<b>40</b>
<b>Centre-Out Task</b> .....	40
<b>ECR Ia Recordings</b> .....	41

Ensemble Average.....	42
<b>3.3 Model Simulations.....</b>	<b>42</b>
Centre-Out Task.....	43
Tendon Displacement Model.....	43
Ia Spindle Models.....	44
<b>3.4 Human and Model Data Comparison .....</b>	<b>45</b>
Qualitative Comparison.....	45
Mean Firing Rate.....	46
Directional Tuning .....	46
Dynamic Index.....	47
Static Index .....	49
Temporal Similarity.....	49
Overall Model Ranking.....	50
<b>CHAPTER 4. RESULTS .....</b>	<b>51</b>
<b>4.1 Qualitative Comparison.....</b>	<b>51</b>
<b>4.2 Mean Firing Rate .....</b>	<b>58</b>
<b>4.3 Directional Tuning .....</b>	<b>59</b>
<b>4.4 Static Index .....</b>	<b>62</b>
<b>4.5 Dynamic Index.....</b>	<b>63</b>
<b>4.6 Temporal Similarity.....</b>	<b>64</b>
<b>4.7 Overall Model Ranking .....</b>	<b>65</b>

<b>CHAPTER 5. DISCUSSION AND CONCLUSION .....</b>	<b>67</b>
<b>5.1 Discussion.....</b>	<b>67</b>
<b>Slower temporal dynamics dominate the models .....</b>	<b>71</b>
<b>Single unit vs. ensemble responses .....</b>	<b>72</b>
<b>Lower background firing rate in humans – difference in static motor drive?.....</b>	<b>72</b>
<b>Rate versus temporal coding.....</b>	<b>74</b>
<b>Limitations of the study .....</b>	<b>75</b>
<b>5.2 Conclusion.....</b>	<b>77</b>
<b>REFERENCES.....</b>	<b>78</b>
<b>APPENDIX - MODEL IMPLEMENTATIONS.....</b>	<b>81</b>
<b>Validation .....</b>	<b>83</b>



## List of Tables

---

<b>Table 4.1.</b> Normalized model errors.....	65
--	----

## List of Figures

---

<b>Figure 2.1.</b> Morphology of the human muscle spindle.....	<b>Error! Bookmark not defined.</b>
<b>Figure 2.2.</b> Response properties of Ia afferents under fusimotor influence.....	<b>Error! Bookmark not defined.</b>
<b>Figure 2.3.</b> Input/Output relationships in black box models .....	27
<b>Figure 3.1.</b> Schematic of experimental protocol. ....	39
<b>Figure 3.2.</b> Matthews' and Modified Dynamic Index. ....	48
<b>Figure 4.1.</b> Comparing movements to opposite targets.....	52
<b>Figure 4.2.</b> Comparing multiple movements to the same target.....	55
<b>Figure 4.3.</b> Comparing models and human ensemble data to two opposing targets.. ....	57
<b>Figure 4.4.</b> Comparing directional tuning in polar plots.. ....	62
<b>Figure 4.5.</b> Comparing model errors for different error categories .....	64

# **Chapter 1. Introduction and Motivation**

---

## ***1.1 Big picture***

The human nervous system can be considered the most complex control system known to man. Since it is at the core of our being and functioning, the desire to understand its complexities is enormous. Further to the pursuit of knowledge, there are many immediate applications that understanding the nervous system can bring. Even with the limited present knowledge, interventions have already been developed to help in many neurological diseases including alleviating tremors in Parkinson's patients by deep brain stimulation (Breit et al. 2004), correcting 'foot drop' (Lyons et al. 2002), and restoring other lost motor function using functional electrical stimulation. The nervous system controls the function of all physiological systems in the body, including respiratory, endocrine, cardiovascular, muscular, and digestive systems. This thesis focuses on the sensorimotor system, which interprets sensation from muscles, tendons, joints and skin, and controls movement via muscular contractions.

### **Basic science perspective**

Currently, interest in the realm of the sensorimotor nervous system is strong. Intact motor control is crucial for everyday movements and therefore the outcomes of research in this area have applications in rehabilitation from acute injury, and congenital and degenerative diseases. The somatosensory system goes

hand in hand with proper functioning of the motor system since reflexes and proprioception are necessary components for smooth motion, and constitute an integral part of the continuous sensorimotor feedback loop. Investigations in this field are closing in on gaps in our understanding of locomotion, reflexes, voluntary movement, development and learning. Afferent sensation from the sensorimotor system, namely proprioception derived from muscle spindles, will be the spotlight for exploration in this thesis.

Why is it that we can easily guide our hand to touch our nose with closed eyes? If our sense of arm position still exists without visual clues, there must be something internal in our bodies keeping track of where we move. This sense of our own position is called 'proprioception' and is crucial in allowing us to precisely and accurately move through space without conscious effort.

Proprioception is derived from specialized receptors in skin, joints, muscles and tendons that constantly provide sensory feedback to the nervous system in response to movement. When muscles move, sensory organs called 'muscle spindles' are activated and send signals related to the state of the muscle to the central nervous system. These responses are crucial to the brain's knowledge of where each limb is in space, and contribute to one's ability to balance and make movements without difficulty.

The aim of this study is to gain a greater understanding of neural encoding from muscle spindles during movement. A large proportion of experimental recordings of muscle spindle afferents have been done in animals, mostly cats. However, with the advent of human microneurography in the late 1960's, insight

into the workings of human muscle spindles began to emerge. At the same time that human microneurography began gaining momentum, the development of quantitative models based on cat muscle spindle physiology started (Matthews and Stein 1969) and continued over the next three decades (Chen and Poppele 1978; Hasan 1983; Houk et al. 1981; Prochazka and Gorassini 1998a; b; Scott and Loeb 1994). To date, the mathematical models of muscle spindle primary afferents have only been tested with data sets acquired in acute and chronic cat experiments (Prochazka and Gorassini 1998a; b). It is our conviction to test whether these cat models can generalize to data collected in human studies. Similarities in general response characteristics to muscle stretch have been noted between cat and human afferents, alongside a glaring difference in background firing rate. However, direct comparison between the species has never been made. This is mainly because protocols for cat and human experimentation are very different, and therefore similar movements at the same speed never been performed in both species during afferent recordings. We have specifically addressed this issue by levelling the playing field and comparing responses during exactly the same simulated movement. To achieve this we used six computational models of cat muscle spindle primary afferents to generate hypothetical cat afferent responses to the same movements generated during human recordings.

From a broader perspective, this study focuses on understanding the sensory mechanisms during movement. Not only does sensory information from muscle spindles contribute significantly to proprioception (Cohen 1999), but they

also provide important feedback needed when learning a new motor task. These results will contribute to breaking the barrier towards a deeper understanding of neural communication, especially in the sensory nervous system.

### **Clinical relevance**

Loss of motor control can be a devastating result of 'neurotrauma': damage to the nervous system usually as a consequence of brain or spinal cord injury. Spinal cord injury occurs in 15 to 40 people per million usually as a result of sports injuries, motor vehicle accidents, and workplace injuries (Sekhon and Fehlings 2001). Brain and spinal cord trauma affects primarily young people, and living without motor function for the rest of their lives is daunting and depressing.

Stroke is another common cause of lost motor control, resulting from the death of brain tissue. Some stroke patients have compromised sense of proprioception.

Annual incidence rates for stroke is between 300 and 500 people per 100 000 in the age range of 45 to 84 years (Sudlow and Warlow 1997). Those living without control over their own movement have difficulty performing the simplest of daily tasks such as grasping or walking, and would therefore see a great improvement in quality of life from any restoration of function.

Current techniques such as functional electrical stimulation and neural prosthetics interact with the nervous system of an injured patient by triggered electrical stimulation of motor nerves, activating a muscle indirectly. The trigger can come from a number of sources including direct input from the user (e.g. by pushing a button), a signal from an undamaged peripheral nerve, or a mechanical

stimulus such as a force sensor on the heel of the foot. Once the trigger goes off, an electrical stimulus will be delivered to the desired muscle or prosthetic causing contraction or pre-programmed movement respectively. Although these techniques are of great value, they usually result in unnatural, jerky movements. There is also a lack of sensory information coming from the injured limb to the central nervous system, and the generated movement is only perceived by visual feedback and an a priori knowledge that the device is in use. In an effort to allow for more natural movements, an area of current development is the incorporation of sensory feedback from proprioceptors, or artificial proprioceptor-like sensors (Gandevia 1996; Prochazka 1996; Stein et al. 2004). This will be the first modeling study on *human* muscle spindles. Muscle spindle afferents are important proprioceptors, and are unique as biological sensors because their transduction properties are modulated in *real-time* or *a priori* given the context of movement by the CNS through fusimotor efferents (Kandel et al. 2000). From a clinical perspective, we hope that the knowledge gained from our study of the sensory coding scheme in muscle spindles will be important for implementation of rehabilitation in humans as well as for developing biomimetic prosthetics. The ultimate goal of research like ours is to gain a thorough understanding of the actual neural encoding pattern used during closed-loop motor control in order to directly communicate with the nervous system in its own language.

## **Unanswered research questions addressed in this thesis**

The CNS uses information from proprioceptors to decode exactly what movement has been made. Prior knowledge of how neural firing rate is encoded is necessary for decoding purposes. Currently there exist predictive models based on muscle spindle response in cats that can determine firing rate according to length and velocity of muscle stretch (Chen and Poppele 1978; Hasan 1983; Houk et al. 1981; Matthews and Stein 1969; Prochazka and Gorassini 1998b). These models have been proven to be effective in fitting data during very controlled cat movements and also fit firing rate profiles during natural cat locomotion (Prochazka and Gorassini 1998b). The role of these models in predicting *human* data has never been elucidated, and that constitutes the major goal of this thesis: Do cat models predict human muscle spindle afferent response during movement?

The underlying question is clear but a meaningful method of evaluation of the models is less obvious. The traditional way of evaluating the fit of a model is to use a least-squared linear regression. Although this provides one measure of ‘goodness of fit’, the error is based on residuals rather than a physiological inaccuracy. Therefore, the more subtle question that is posed in this thesis is: Do the cat models predict *physiological* measures of human muscle spindles? If so, which of these measures is best represented in each model? The physiological measures that will be tested are instantaneous (temporal) fidelity, dynamic and static indices, mean firing rate, and directional tuning. All measures are weighted equally in our evaluation; the measure(s) of most significance in the central



nervous system is not clear and thus we do not attempt to put more or less importance on any one measure.

There is one clear discrepancy between the cat and human data that is the high level of background firing rates in cats (50 to 110 imp/s), and the much lower activity found in humans (8-12 imp/s). The difference is speculated to arise from a high level of tonic gamma static motor neuron activity in cat experiments (Prochazka and Gorassini 1998a; b). Although this has not been confirmed as the differentiating factor between cats and humans, neither static nor dynamic fusimotor activity has been included in our simulations and thus this will not be explored. Model evaluations will be done after simply subtracting an offset to bring the baseline down to the order of human rates.

Our emphasis is on a first order assessment of the applicability of these models to human data, in the hopes that these models can one day be useful in clinical human neurorehabilitation. Our hypothesis is that cat and human spindles are similar enough in morphology that the current predictive models will be transferable to humans albeit with limited accuracy given that they were developed from a limited dataset from another species.

## ***1.2 Primary methodological approach in the thesis***

A brief overview of the experimental protocol is delivered in this section. Details will be provided later in the full-length Methodology section.

## **Experimental Data**

The experimental data in this thesis were obtained in previous studies (Jones *et al.*, 2001). Microneurographic recordings of muscle spindle afferents were done while subjects performed a centre-out task. Eight primary spindle afferents from the ECR (extensor carpi radialis) muscle were chosen for inclusion in this study. The kinematic movement trajectory of the hand in 3D space was simultaneously captured.

## **Modelling**

The human data was compared to the predictions of six cat muscle spindle primary afferent models (Chen and Poppele 1978; Hasan 1983; Houk *et al.* 1981; Matthews and Stein 1969; Prochazka and Gorassini 1998a; b). Using Matlab simulation software, the six models were implemented as found in the Prochazka and Gorassini study, with the same parameters that gave the best fit to the ensemble firing rate for nine hamstring spindle primary afferents during normal locomotion in chronic cat experiments (Prochazka and Gorassini 1998b). We do not consider the effect of fusimotor drive in our study. The kinematics corresponding to the human data were averaged and converted to ECR muscle stretch using a tendon excursion model of the wrist (Loren *et al.* 1996). These simulated muscle stretches, corresponding to the human movement during the centre-out task, were input into the spindle afferent models to produce predicted firing rates that could then be compared to the recorded human rates.

## **Analysis**

The six model predictions were compared to the ensemble human recordings. Correspondence between qualitative characteristics of firing patterns were noted as the general shape of the instantaneous firing rate time course was similar in both human and model spindle afferents to each centre-out target. A root mean square error between each model and the human data was then computed for five physiologically relevant categories: preferred direction, sharpness of tuning, temporal similarity, dynamic index, static index. All quantitative measurements are reported to identify the strengths and weaknesses of each model. A final ranking order of the ‘predictive ability’ of the six models is produced by collapsing the performance in each category to one overall score for each model.

### ***1.3 Thesis organization***

The thesis is organized into chapters. The following chapter (Background and Literature Review) is the longest and contains an introduction to basic concepts that are crucial to understanding this study. Proprioception, muscle spindles, cat afferent models, and analysis methods are discussed in more detail in that section. Chapter 3 is the Methodology, and briefly goes over the experimental paradigm and outlines in detail how the analysis was performed. The Results section, Chapter 4, concisely lays out the qualitative and quantitative comparisons made between the models and ensemble human data, using figures and tables to illustrate and summarize results. The Discussion in Chapter 5 attempts to interpret the results in context of current scientific knowledge, with a particular

focus on comparing these human-based results to those found in the Prochazka and Gorassini cat based study (Prochazka and Gorassini 1998b). Finally, the Appendix is included for those readers interested in the details of implementation of the muscle spindle models in the Matlab/Simulink environment.

## **Chapter 2. Background and Literature Review**

---

This section will outline background material pertinent to the thesis. The sense of proprioception and muscle spindles will be discussed in the context of anatomy and physiology with reference to important scientific findings in the literature. A summary of each spindle model analyzed in the thesis will also be presented, along with specific methods of data analysis and details of the experimental paradigm.

### ***2.1 Proprioception***

#### **A Sixth Sense**

Proprioception is often referred to as our ‘sixth sense’. The term was first coined by Nobel laureate Sir Charles Sherrington in the early 20<sup>th</sup> century (Smetacek and Mechsner 2004) and is often used interchangeably with the word kinaesthesia. It describes the sensation of knowing where our limbs are in space; this normally occurs without conscious thinking. Even when visual perception is removed our sense of position remains, supporting the idea that proprioception is an autonomous internal sense. Without this, one would find it very difficult to balance or make voluntary movements because there would be no sense of initial limb position from which to derive the desired movement. Proprioception, in conjunction with the perceptions from the vestibular and visual systems, provides the necessary control feedback to stand up straight without falling over.

Sensation is traditionally thought to originate from external stimuli, which activate specialized receptors that send signals to the brain to be centrally processed. For example, photoreceptors on the retina translate light into neural signals which the brain processes as vision, cutaneous receptors in the skin respond to touch, the cochlea responds to auditory stimuli and so on. In the case of proprioception, instead of external stimuli, proprioceptors respond to internal changes of our own body, such as muscle or skin stretch, or joint movement.

Most people who suffer loss of proprioception also have motor deficits, usually as a result of stroke, spinal cord, or brain injury. Furthermore, stroke patients with somatosensory deficits recover motor function slower than those without (Reding and Potes 1988). The extent of the sensory and motor deficiency is dependent on the site of the injury. Although rare, it is possible to have a generalized purely somatosensory deficit, although the origins of such diseases are not well classified. Examples of patients who have suffered major proprioceptive deficit include Ian Waterman who completely lost the ability to coordinate movement after a viral infection (Cole 1995), and Christina, the disembodied lady described by Oliver Sachs who felt completely disconnected from her own limbs (Sachs 1985). Both of these individuals were able to regain some control over their body, but only after meticulous training in usage of their visual system to compensate for their sensory loss.

So exactly where are these sensory receptors that generate proprioception located, and what is the evidence that they exist? This question will be addressed in the next section.

## **Types of Proprioceptors**

From the 1960's through the 1980's there was an ongoing discussion as to which internal receptors were responsible for relaying information about movement to the central nervous system. Three possible mechanoreceptors had been identified; those in the skin (cutaneous receptors), joints (joint receptors) and muscle (muscle spindles) all seemed plausible.

Historically it had been thought that joint receptors were the main sensors involved in proprioception. However in 1972 a novel experiment challenged this view when differences in sensations derived from excitation of muscle and joint receptors were evaluated (Goodwin et al. 1972a). Vibration over the tendon of a muscle is known to have the ability to excite muscle spindle afferents. In a matching task, blindfolded subjects were asked to use their right arm to track the position of the left arm, which had been moved passively by the experimenter. When the biceps of the right arm was vibrated, the error in tracking prediction would increase such that the biceps of the tracking arm was stretched in relation to the reference arm. The same experiment done with vibration over the joint did not produce these errors in prediction. This was indicative that muscle spindle activation could provide illusory sensations of muscle stretch while activation of joint receptors did not seem to distort proprioceptive perception (Goodwin et al. 1972a). Furthermore, anaesthesia of joints and skin still allowed for movement detection of the affected limbs, presumably due to feedback from still functioning muscle spindles (Goodwin et al. 1972b).

These experiments do not however completely exclude the role of joint and cutaneous receptors in kinaesthesia. When muscle spindles are the only afferents available, although movement is detected, prediction of limb position is significantly compromised in comparison to when all three receptors are functioning (Gandevia et al. 1983; Gandevia and McCloskey 1976). It is likely that joint and cutaneous receptors serve to facilitate information from the muscle spindles, especially at the extremes of joint rotation when the slowly adapting joint and cutaneous receptors are most active (McCloskey 1995).

Another sensory organ in the muscle, the Golgi tendon organ (GTO), was not included in the above discussion for specific reason. GTOs are found at the junction between tendon and muscle and are thus in series with muscle. They only respond when the muscle is tense or contracted, requiring voluntary muscle activation for a response. Therefore since feedback information is only available during voluntary (active) rather than involuntary (passive) movements, GTOs would not provide the complete picture necessary for proprioception. Rather, they serve as a good mechanism to track the tension in the muscle, which is proportional to the voluntary motor drive of the central nervous system to the muscle in question (Stein 1980).

## ***2.2 Muscle Spindles***

This thesis explores the similarities and differences between cat and human muscle spindles. Specifically, we focus on evaluating the response properties of a group of sensory neurons, classified as Ia afferents, during movement. Therefore



a brief background of muscle spindles in regards to distribution and morphology will be presented, followed by a detailed discussion of the response properties of the spindle afferents.

## **Distribution**

Muscle spindles are located throughout striated muscle tissue and are generally positioned in parallel with extrafusal muscle fibres. The number of spindles per muscle varies and is thought to be greater in muscles requiring precision of fine movement. In 1971, Voss tabulated work done by him and others that quantified the number and density of spindles in various human muscles (Voss 1971). Large muscles in the leg such as the gastrocnemius and quadriceps femoris have a relatively low spindle density, with just 0.4 spindles/g and 0.8 spindles/g respectively (Voss 1971). More recent studies show that muscles in the neck are some of the densest known areas for muscle spindles in humans, with densities ranging from 24 to 43 spindles/g (Boyd-Clark et al. 2002). Interestingly, it has also been shown that the shorter, smaller muscle of a parallel agonist pair generally has a higher proportion of muscle spindles in both dogs and humans (Boyd-Clark et al. 2002; Peck et al. 1984). Wrist muscles are of primary interest in this thesis and have densities that range from 2 to 5 spindles/g, greater than leg muscles but lower than both neck and finger muscles. Specifically, the extensor carpi radialis brevis (ECRb) of the wrist will be the focused on in our study and has a spindle density of 3.2 spindles/g, or approximately 102 spindles per muscle (Kokkorogiannis 2004).

## **Morphology**

### ***Shape and Size***

A typical muscle spindle is fusiform in shape, 8-10mm long in cats and 6-8mm long in humans (Boyd 1985). A cartoon schematic of a typical spindle is seen in Figure 2.1.

### ***Intrafusal fibres***

Each spindle is comprised of a small group of intrafusal fibres innervated by efferent and afferent axons, surrounded by an endothelial-like spindle capsule that acts as protection from the external environment. Three types of intrafusal fibres have been identified: bag1, bag2 and chain. Most spindles have one bag1, one bag2, and 4-8 chain fibres (Boyd 1985). Thirty percent of human spindles contain an extra bag1 or bag2 fibre, and some contain up to four bag and up to eleven chain fibres (Boyd 1985). Bag fibres are about 2.4mm longer than the length of the capsule and tend to stick out at the ends, while chain fibres are shorter and tend to be contained within the capsule (Boyd 1985).

**Figure 2.1 has been removed due to copyright restrictions.**  
Please refer to *Kandel et. al, 2000, pg. 719*

The distinguishing feature between bag and chain fibres is the arrangement of nuclei along the equator of the fibre. Intrafusal fibres are single cells that have multiple nuclei as a result of their conception from several myoblasts fusing during development. In chain fibres, nuclei tend to be lined up in a single column along the length of the fibre, while in bag fibres the highest density of nuclei is at the equator such that if cut transversely there, more than one nuclei will be encountered (Matthews 1972).

Myofibrils lie mostly in the polar regions of intrafusal fibres, as the equator remains non-contractile while the poles are contractile. The compositions of sarcomeres within myofibrils tend to differ between bag and chain fibres thus

giving rise to different mechanical properties in intrafusal fibres: bag1 is considered slow-acting, bag2 intermediate, and chain fast (Proske 1995). Chain fibres are known to be strictly elastic, while there is evidence of a viscous element in the poles of nuclear bag fibres along with elasticity. A viscous element implies velocity sensitivity may exist in bag fibres, whereas strict elasticity in chain fibres only allows for displacement sensitivity (Matthews 1972).

### ***Afferent Innervation***

There are two types of myelinated sensory afferents in the muscle spindle: primary (Ia) afferents, and secondary (II) afferents. Ia afferents have a diameter of about 12 to 20  $\mu\text{m}$  and group II afferents are slightly smaller, with diameters ranging from 4 to 12  $\mu\text{m}$  in cat hindlimbs (Hunt 1954). Primary afferents branch out and innervate all intrafusal fibre types by spiralling their endings around the equator as illustrated in Figure 2.1. Type II afferents predominantly innervate bag1's and chains, and only rarely are known to interact with bag2's (Stein 1980). Secondary afferents innervate closer to the poles of the intrafusal fibres, and have spray endings on bag1's and spiral or spray endings on chains (Matthews 1972). There are typically one to two Ia endings and one to five type II endings that innervate each spindle (Prochazka 1996). Since Ia's and II's differ in the types of fibres they innervate, and these fibres have different viscoelastic properties, it is not surprising that the afferents also differ in their response properties. Differences in afferent response characteristics will be discussed in detail shortly.

### ***Efferent Innervation***

Muscle spindles are unique as sensory receptors because the CNS has specialized control over their mechanical properties through the *fusimotor system*. This system is comprised of myelinated efferents that innervate intrafusal fibres and consists of  $\beta$ -skeletofusimotor (large-diameter) and  $\gamma$ -fusimotor (small-diameter) axons.  $\beta$  fibres are skeletomotor axons that innervate extrafusal fibres, but also branch and simultaneously innervate intrafusal fibres.  $\gamma$ -axons strictly innervate intrafusal fibres.

Within the fusimotor system, efferents are labelled either as static or dynamic depending on the type of fibre they innervate. Dynamic  $\beta$  and  $\gamma$  axons have motor plate endings on the contractile (polar) regions of bag1 intrafusal fibres. Bag1 fibres are noted for their velocity sensitivity due to their viscoelastic properties and thus efferents associated with them are labelled 'dynamic'. Bag2 and chain fibres are known to be sensitive only to displacement.  $\beta$  and  $\gamma$  axons that have motor plate endings on the contractile (polar) regions on one or more bag2 and chain fibres are known as 'static' (Prochazka 1996).

Activation of the dynamic fusimotor system will cause contraction of bag1 fibres, thus increasing the tension and therefore increasing the response rate of the type Ia afferents which innervate bag1's. Activation of a static  $\gamma$  or  $\beta$ -motor neuron causes contraction of bag2 and chain fibres, and thus increases the responses of both type Ia and II afferents that innervate them. The fusimotor system therefore acts as a centrally modulated 'sensitivity control' for muscle

spindle afferent firing rate. The implications of this 'sensitivity control' on afferent responses are explored in the next section.

### **Response Properties**

Muscle spindles are *mechanoreceptors*, meaning that their response is generated by a mechanical change in structure. When the muscle is stretched the spindles stretch correspondingly. This change in length of the intrafusal fibres causes the afferent endings to be extended and leads to an increase in firing rate. Muscle spindles therefore transfer a measure of muscle stretch to the central nervous system (CNS). The CNS also has control over the sensitivity of these stretch receptors via the fusimotor system. When fusimotor axons are activated, their endings pull on the ends of the intrafusal fibres causing the central region to stretch, thus instigating a higher firing rate in the afferent neurons without an overall stretch of the muscle. We will now discuss the known firing response characteristics of the two types of muscle spindle afferents. Responses have been well characterized by a number of studies in the cat, human, and monkeys and are found to be quite similar across species (Prochazka 1996). The descriptions below describe the general firing rate characteristics of both Ia and II afferents in response to movement.

#### ***Secondary afferent response***

Secondary afferents are known to be primarily length-sensitive. During a ramp-and-hold stretch with constant fusimotor input, group II afferents respond with a continuous increase in firing rate until the stretch reaches completion. There are

some instances where secondary afferents also display velocity sensitivity, i.e. at the onset and release of a stretch a sudden jump or drop in firing rate will be noted instead of a continuous change. However, as a general rule the velocity dependence seen in secondary afferents is negligible when compared to that of primary afferents (discussed below). The length-sensitivity of secondary afferents is not surprising when considered in the context of spindle anatomy. Only chain and bag2 fibres are innervated by group II's and have mainly elasticity to overcome during stretch. Therefore, the deformation in these intrafusal fibres, and in turn the resulting firing rate, should be directly proportional to the stretch applied (Matthews 1972).

### ***Primary afferent response***

Primary afferents are length-sensitive just as secondary afferents, but they also show velocity sensitivity. When a ramp-and-hold stretch is applied to a muscle and Ia's are recorded from, the onset of movement is accompanied by a burst of high frequency spikes that settles to a level well above baseline firing (velocity dependence), before increasing firing rate in a ramp-like fashion proportional to the rate of stretch (length dependence). All of these features can be seen in the first firing rate trace for Ia's in Figure 2.2. It is thought that the viscous nature of the bag1 fibres innervated by primary afferents is what accounts for the velocity sensitivity in Ia's that is absent in II's (Matthews 1972).

Both primary and secondary afferents have a 'linear range' in which their length sensitivity (measured as the amplitude of firing rate divided by the

amplitude of stretch during sinusoidal movements) increases as the stretch becomes larger (Matthews 1972). The linear range for primary afferents is less than 0.5% of muscle rest length (Prochazka 1996), whereas the secondary afferent sensitivity remains linear for most of the muscle range of motion.

### ***Influence of fusimotor system***

The responses described above are the typical profiles seen from muscle spindle afferents during a *constant* input level from the fusimotor system. However, since the system is under direct control by the central nervous system, it is important to understand the effects of a change in fusimotor drive on afferent responses.

Experimental investigations focus on the effects of the  $\gamma$ -fusimotor system because  $\beta$  fibres are not necessarily uniformly present in all spindles (Matthews 1972). The work thus far has characterized how activity from the  $\gamma$ -static and  $\gamma$ -dynamic efferent systems changes firing responses in Ia and II afferents during controlled movement.

In the linear range of muscle spindle afferent sensitivity (described in the previous section), increasing activity of the fusimotor static drive has the effect of lowering the sensitivity of secondary afferents, while increasing dynamic drive will increase Ia sensitivity (Matthews 1972; Prochazka 1996).

This thesis focuses on movements that are larger in amplitude ( $>0.5\%$  rest length), and are likely outside the linear range. Figure 2.2 shows the effects of static and dynamic fusimotor drive on the primary afferent firing rate during a ramp-and-hold muscle movement. During  $\gamma$ -static stimulation the overall



response from Ia's has the same shape as without stimulation, but with an added offset in baseline firing rate. The effect of  $\gamma$ -dynamic stimulation on the Ia afferent is to accelerate the rate at which firing rate increases in response to the positive stretch; effectively the gain has been increased.  $\gamma$ -dynamic stimulation appears to have little effect on type II afferents. When both static and dynamic fusimotor are applied, a superposition of the effects are seen; in Ia's the offset and gain are increase and in II's only the offset is increased (Prochazka 1996).

**Figure 2.2 has been removed due to copyright restrictions.**  
Please refer to *Kandel et. al, 2000, pg. 719*

The functional significance of the fusimotor system could be to ensure afferent responsiveness during the entire muscle range of motion. For instance, shortening

of the extrafusal muscle fibres will unload muscle spindles causing the afferents to become silent. In order for the CNS to derive information about muscle shortening, it would be required that the muscle spindles still be active in this position. Therefore, fusimotor activation under these conditions will cause contraction of the intrafusal fibre poles, thereby stretching the intrafusal sensory regions and allowing them to continue transducing information.

The amount of fusimotor modulation is task-dependent. In studying afferent activity in cats while performing a variety of tasks, it was shown that static and dynamic fusimotor drive increased as the speed and difficulty of the task increased (Kandel et al. 2000). Specifically, when the cat was in unpredictable situations during imposed movements, dynamic gamma activity increased. These results suggest that the activity of the fusimotor system is modulated by the CNS to reflect the amount of information needed during tasks of varying difficulty.

### ***2.3 Computational Models***

Modelling is a common tool used in scientific fields to mimic a process of interest. Models come in many different forms including physical, conceptual, and computational. Computational models are of particular value because they provide a mathematical basis that relates input to output, quantifying the output in terms of the input. This property allows computational models to be used in simulations in order to gain better insight into processes that might not otherwise be possible through experimental means alone.

## **Examples of Modelling in Physiology**

There are countless examples of modelling used in physiology to understand bodily functions. Biomechanics is one example of a huge field that uses mechanical elements such as springs and dampers in conjunction with force, kinematics and mathematics to model the behaviour of muscle, joints, tendon, and bones during movement. Human gait analysis is often performed in the clinic to identify abnormalities in walking; this is made possible by comparing a normal gait model to the patient in question (Enderle 2000). Another application of biomechanics is in total knee replacement surgery. Biomechanical models of the knee are also currently being investigated as a tool to use in surgery to ensure that correct tension and balance in the tendons are achieved in the new knee.

Neuroscience is another field in which computational models have become paramount. Hodgkin and Huxley became famous by the introduction of their circuit model of a patch of cell membrane. Electrical elements such as resistors and capacitors are used to represent ion conductances and membrane properties. This model is ubiquitously known and applied throughout computational neuroscience to model action potential generation under different conditions.

In this thesis we use muscle spindle models and simulations to seek answers to our question of whether human and cat muscle spindle afferents have similar response properties.

## Muscle Spindle Models

Experimental evidence has made it clear that muscle spindle afferents respond in a rather predictable way in response to muscle stretch and velocity. This has led to the proposal of a number of mathematical models that attempt to quantify the relationship between muscle movement and spindle afferent firing rate (Chen and Poppele 1978; Hasan 1983; Houk et al. 1981; Matthews and Stein 1969; Prochazka and Gorassini 1998b). The models that have been proposed are all based on data derived from cats. It is our conviction to apply these models to human data in order to see if cat muscle spindle models can generalize to human spindles. The focus of our work will be on primary (Ia) afferents.

The six primary afferent models of interest all take muscle stretch (or equivalently tendon displacement) as input, and convert that into instantaneous firing rate. From now on we will refer to muscle stretch input as  $x(t)$  and firing rate output as  $f(t)$ . We can think of each of the models as a ‘black box’ that contains a transformation function  $h(t)$  that makes the change from  $x(t)$  to  $f(t)$ . In the time domain, input is related to output by the following convolution:

$$f(t) = h(t) * x(t)$$

Sometimes it is easier to think of the relationship in the frequency domain since there is no convolution involved but rather a straight multiplication between the model transfer function  $H(s)$  and the input:

$$F(s) = H(s)X(s)$$

Switching between the time and frequency domains is simply done by using a Laplace transform, as shown in Figure 2.3.

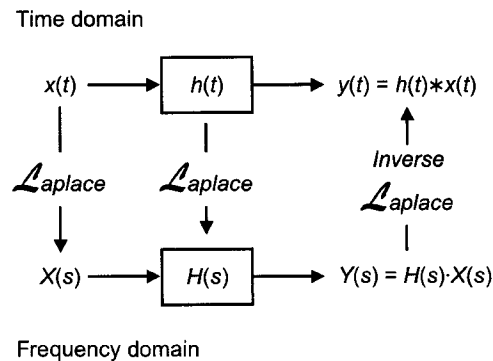


**Figure 2.3. Input/Output relationships in black box models.** A general illustration showing the relationship between input  $x(t)$ , output  $y(t)$  and a given model  $h(t)$ . The relationship can be considered both in the time and frequency domains, which are related by a simple Laplace transform. In our study, the muscle spindle model will be represented by  $H(s)$  or  $h(t)$ , the input will be tendon displacement and the output firing rate. *Image source (Wikipedia online)*

### ***Spindle Model Simplifications and their Implications***

There are inherent assumptions and simplifications in any model that describes a process that is not fully understood. This is necessary both to limit complexity and also to fill in holes that the current knowledge base cannot. When using a model, it is essential to understand the full implications behind the model assumptions.

All of the primary afferent spindle firing rate models that we are dealing with in this thesis have instantaneous firing rate as their output. If the output were to be used to interpret coding and decoding mechanisms, it would be presumed that the unit important to the nervous system is indeed *firing rate* rather than individual *spike times*. These models thus imply that rate encoding

dominates over temporal encoding in muscle spindle afferents. Whether this is true or not has not been fully elucidated, though it is generally accepted that rate coding prevails in the peripheral nervous system and temporal encoding plays a larger role in the central nervous system.

Another property that these models share is their deterministic nature. That is, exactly the same output will be faithfully produced from a given input. This assumes that muscle spindle afferents also encode muscle stretch and velocity deterministically, without ambiguity. Stochastic models use random variables to determine output from a probabilistic function. This is an alternative means that might be closer to the way in which the nervous system functions, although until now this has not been proven.

### **Comparison of the six models in cats**

A landmark study that compared six accepted spindle primary afferent models in the literature was performed by Prochazka and Gorassini in 1998 (Prochazka and Gorassini 1998b). Spindle primary afferents were recorded during normal cat locomotion. During the step cycle, muscle stretch was also monitored using a length gauge to measure tendon displacement. This data was consolidated and used to fit the model parameters to best predict firing rate from muscle movement. The six models that were evaluated include the models proposed by Matthews & Stein, Houk et al, Chen & Poppele, Hasan, and two models by Prochazka and Gorassini (referred to as P&G1 and P&G2 from now on). The reason this study was so influential was because it fit the models to *natural* movements in behaving

cats. Most of the models were originally based on very controlled movements, such as ramp-and-hold or sinusoidal stretches. The ability for the models to make the transition from controlled to natural movements was indeed impressive. The results of the comparative study showed that the Chen & Poppele, Hasan, and P&G2 models performed best when predicting primary afferent firing rate in response to cat locomotion (Prochazka and Gorassini 1998b).

### **Six Firing Rate Models**

It is important to understand the basis behind each of the primary afferent firing rate models in order to identify strengths and weaknesses of each model after the final evaluation has been made. Therefore a short summary of the experiments and the mathematics behind each of the evaluated models are presented here.

Some of the models are best understood in the time domain, while others are best understood in the frequency domain. Models will be presented in the most intuitively comprehensible form.

#### ***Prochazka & Gorassini 1***

Prochazka and Gorassini developed two simple models based on fits to their cat locomotion data. Their data showed a strong dependence of instantaneous firing rate on the velocity of muscle stretch. Therefore, the first model they proposed for Ia afferents was dependent only on velocity, raised to the exponent 0.6. The form of the model is as follows:

$$f(t) = k_1 + k_2 \left( \frac{dx(t)}{dt} \right)^{0.6} \quad (\text{Prochazka and Gorassini 1998b})$$

where  $k_1, k_2$  are fitted parameters of 82 and 4.3 respectively  
 $f(t)$  is instantaneous firing rate  
 $dx(t)/dt$  is instantaneous muscle velocity

### ***Prochazka & Gorassini 2***

The second model by Prochazka and Gorassini simply added a length dependent component to the first equation, such that the new model is of the form:

$$f(t) = k_1 + k_2 \left( \frac{dx(t)}{dt} \right)^{0.6} + k_3 x(t) \quad (\text{Prochazka and Gorassini 1998b})$$

where  $k_1, k_2, k_3$  are parameters fitted as 82, 4.3, and 2 respectively  
 $f(t)$  is instantaneous firing rate  
 $x(t)$  is instantaneous muscle length  
 $dx(t)/dt$  is instantaneous muscle velocity

### ***Houk et al***

The experiments of Houk and colleagues focused on the dynamic response of Ia afferents. Recordings were made from primary afferents in the soleus muscle of decerebrate cats. Ventral roots were still intact allowing for spontaneous fusimotor drive. A series of large amplitude (10mm) ramp and hold stretches were applied to the soleus muscle at velocities ranging from 0.4 to 100 mm/s (Houk et al. 1981). Ignoring the bursting activity often seen in spindle primary afferents at the onset of a ramp and hold stretch, they were able to fit a nonlinear model to their data.



The model they proposed was muscle length and velocity dependent, but instead of the terms being additive, Houk et al proposed that they were multiplicative. They suggested that firing rate increases from a baseline rate proportional to the multiplication of length and velocity terms. The equation of the model as used in the Prochazka and Gorassini study is:

$$f(t) - f_o = K(x(t) - x_o) \left( \frac{dx(t)}{dt} \right)^{0.3}$$

where  $f_o$ ,  $x_o$ ,  $K$  are parameters fitted as 82, 0.6, and 25 respectively  
 $f(t)$  is instantaneous firing rate  
 $x(t)$  is instantaneous muscle length  
 $dx(t)/dt$  is instantaneous muscle velocity

### ***Matthews & Stein***

Matthews and Stein applied sinusoidal stretches from 0.03 to 300 Hz to the soleus muscle of decerebrate cats with intact spontaneous fusimotor activity. Recordings were made from primary spindle afferents as the stretches were applied.

Sensitivity of Ia afferents was measured as the amplitude of the response (imp/s) divided by the amplitude of the stretch (mm). The findings showed a distinct linear range for Ia afferents in which their sensitivity to stretch increased proportionally to amount of stretch applied, up to a stretch amplitude of 0.1 mm (Matthews and Stein 1969). A clear relationship between sensitivity and frequency of stretch was also found within this linear range, where the response of the ending could be characterized by the vector sum of the length and velocity components of stretching (Matthews and Stein 1969). For low frequencies (less

than 1Hz), the response was mostly weighted by the length component, whereas at higher frequencies (1Hz up to 30Hz) the velocity contributions became more apparent.

The authors showed that the data from their primary afferents within the linear range could be captured by this equation in the frequency domain:

$$F(s) = \frac{K}{W}(s + W)X(s) \quad (\text{Matthews and Stein 1969})$$

where  $F(s)$  is the response of the primary afferent in the frequency domain

$X(s)$  is muscle length in the frequency domain

$K$  is the sensitivity of the ending at low frequencies

$W$  is the corner frequency where length and velocity components are equal

In the time domain, the additive, weighted contribution of muscle length and velocity components becomes more apparent:

$$f(t) = Kx(t) + \frac{K}{W} \frac{dx(t)}{dt}$$

where  $K$ ,  $W$  are sensitivity and corner frequency parameters respectively

$f(t)$  is instantaneous firing rate

$x(t)$  is instantaneous muscle length

$dx(t)/dt$  is instantaneous muscle velocity

A corner frequency ( $W$ ) 1.5Hz and low frequency sensitivity ( $S$ ) of 95 imp/s/mm were the values fitted to the authors' dataset. The corner frequency was changed to 10 rad s<sup>-1</sup> (approximately 1.6Hz) in the Prochazka and Gorassini simulations and in our study (Prochazka and Gorassini 1998b). When considering the results of this model in the context of this thesis, it is important to keep in mind the

requirement that the afferent be responding to stretches within the linear range (<0.1mm).

### ***Chen & Poppele***

Chen and Poppele evaluated primary afferent responses to small amplitude sinusoidal stretches of cat tenuissimus and triceps surae muscles under controlled fusimotor activation (Chen and Poppele 1978). From these results they were able to empirically derive a transfer function that could mimic primary afferent responses during small amplitude stretches:

$$H(s) = \frac{Ks(s+11)(s+0.4)(s+44)}{(s+0.04)(s+0.8)}, \text{ where K is a gain constant}$$

*(for small amplitude stretches)*

The model above is not valid for large amplitude stretches because spindle sensitivity to length does not increase linearly after a certain threshold of stretch amplitude (0.1 mm). However, Chen and Poppele also fitted data for a large amplitude stretch of 6mm at rate 5mm/s, to a new transfer function, which required one zero, s+11, to be changed to s+4:

$$H(s) = \frac{Ks(s+0.4)(s+44)(s+4)}{(s+0.04)(s+0.8)}, \text{ where K is a gain constant}$$

*(for large amplitude stretches)*

Therefore, although it was confirmed that non-linearities indeed exist in the responses of primary afferents to muscle stretch, it is possible to model the response with a linear transfer function for a small range of stretch amplitudes

where the response will stay relatively linear. The large amplitude version of the primary afferent model was used by Prochazka and Gorassini in their study, with slight alterations after fitting to cat locomotion data. Their modified model is what will be used in this thesis:

$$H(s) = \frac{20.52s(s + 0.4)(s + 44)(s + 4)}{(s + 0.04)(s + 0.8)(s + 200)(s + 200)}$$

### ***Hasan***

The model proposed by Hasan is unique because its inspiration came from theoretical rather than empirical origins (Hasan 1983). The objective was to develop a model that was based on the morphology of the muscle spindle. The resulting model was tested against both small amplitude sinusoidal stretches and large ramp and hold stretches. Here we present a brief summary of the development of the set of differential equations belonging to the Hasan model.

Let  $\mu(t)$  be proportional to the elongation of the sensory zone of an intrafusal fibre. Based on muscle spindle afferent properties, firing rate must be proportional to both the length and velocity of sensory zone elongation so it is reasonable that:

$$f(t) = h(\mu(t) + p \frac{d\mu(t)}{dt}) \quad (1)$$

where  $h$  and  $p$  are proportionality constants

Now if we let  $x(t)$  be the length of the entire intrafusal fibre that the primary afferent innervates, and  $w(t)$  be the length of the non-sensory part of the fibre, then  $x(t)$  must be the sum of the sensory and non-sensory zone lengths:

$$x(t) = w(t) + \mu(t) \quad (2)$$

Now consider the force  $g(t)$  in the intrafusal fibre. The sensory zone is assumed to only have elastic properties and thus the amount of force in this area must be proportional to elongation of the sensory zone:

$$g(t) = k\mu(t) \quad (3)$$

where  $k$  is the elasticity constant of the sensory zone

The force in the non-sensory zone of the fibre is more complicated since this zone has both viscous and elastic properties. The force can thus also be represented as:

$$g(t) = E(w(t) - c) \left( 1 + \left( \frac{1}{a} \frac{dw(t)}{dt} \right)^{1/3} \right) \quad (4)$$

where  $E$ ,  $c$ ,  $a$  are constants

By combining equations (2), (3), and (4), we get:

$$\frac{d\mu(t)}{dt} + a \left( \frac{b\mu(t) - x(t) + c}{x(t) - c - \mu(t)} \right)^3 = \frac{dx(t)}{dt} \quad (5)$$

where  $a$ ,  $b$ ,  $c$  are constants, and  $E$ ,  $k$  have been collapsed into  $b$

If muscle stretch is thought to be equivalent to intrafusal fibre elongation, then equations (1) and (5) give the full description necessary to relate muscle stretch input  $x(t)$  to instantaneous firing rate  $f(t)$ .

Parameters  $a$ ,  $b$ ,  $c$ ,  $h$ ,  $p$ , are selected based on observations from stretch responses and suggested values are given in the Hasan paper. Hasan tested his model against large and small ramp-and-hold, and small sinusoidal stretches with success (Hasan 1983). The parameters used in the Prochazka and Gorassini simulations were  $a=280$ ,  $b=100$ ,  $c = -41$ ,  $h=200$ ,  $p=0.1$ . The simulations in Prochazka and Gorassini modified the model slightly by changing the 0.3 velocity exponent in equation (4) to 0.6 for better performance (Prochazka and Gorassini 1998b). In our study the model was implemented exactly as in the Prochazka and Gorassini paper.

### **Using the Models in this Thesis**

This thesis will use these models with the same parameters as fitted in the Prochazka & Gorassini study to compare their responses to *human* movements. The only change that will be made is in the offset rate, as the background firing rate in cats seems to be significantly higher than in humans. By leaving the parameters unchanged effectively we are trying to answer the question: do spindle primary afferents in cats have the same firing rate characteristics as humans?

Legend for rest of thesis: red – Chen & Poppele, yellow - Houk et. al, orange – Matthews & Stein, purple – Hasan, blue – Prochazka & Gorassini 2, green, Prochazka & Gorassini 1.

## Chapter 3. Methods

---

### 3.1 Overview

The main objective of this work was to determine if any of the six cat Ia muscle spindle afferent models have predictive ability for human Ia afferents. These models have been evaluated in relation to natural movements during cat locomotion and exhibited good fits to ensemble firing rate profiles of cat Ia afferents (Prochazka and Gorassini 1998a; b). To address this issue, we developed simulations to parallel previous human experimental work in order to compare model predictions to actual human afferent output. The overall experimental design is schematically represented in Figure 3.1.

In the human experiments, subjects performed a centre-out task while kinematics of the wrist and neural responses from extensor carpi radialis (ECR) Ia afferents were recorded. The kinematics of the wrist movements were simplified to rotations about two orthogonal and intersecting axes. The movements were measured in degrees with respect to a neutral position defined as the origin of a co-ordinate system with flexion/extension movements along the x-axis (extension being positive) and radial/ulnar deviation movements along the y-axis (radial deviation being positive). This Cartesian system was transformed into a polar co-ordinate system. In the polar system pure extension movements pointed toward the right at 0 deg, pure flexion movements to the left at 180 deg, radial deviation

movements pointed upwards at 90 deg and ulnar deviation movements pointed downwards at 270 deg (Figure 3.1, left).

Simulations with the spindle models were designed to mimic the task performed by the human subjects. The resulting rotations of the wrist recorded during the centre-out task were input into a model of tendon displacement for the ECR muscle (Loren et al. 1996). The tendon displacement output was then used as input into the six different muscle spindle models to generate predictions of Ia afferent firing rate. These predicted rates were subsequently compared both qualitatively and quantitatively to the real human ensemble rates to measure for similarities and differences.



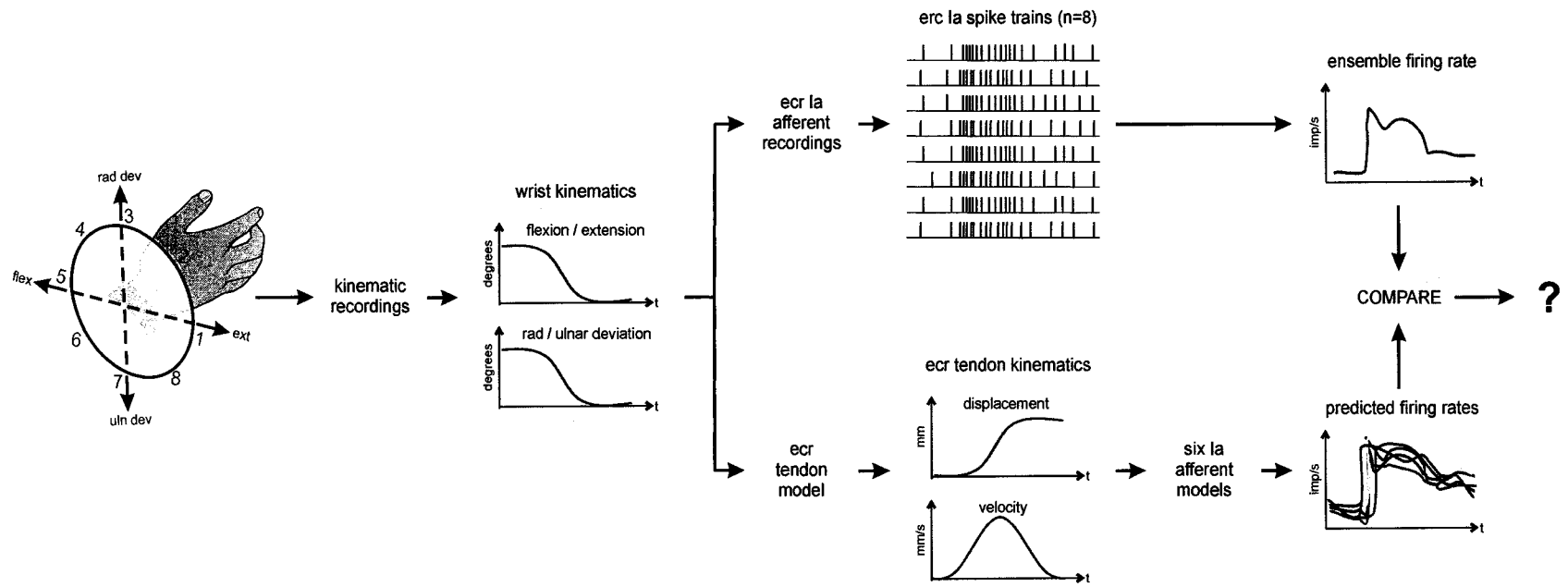


**Figure 3.1. Schematic of experimental protocol.** Human experiments were paralleled with model simulations in order to assess Ia afferent model predictive ability. Subjects performed the centre-out task to eight equally spaced targets around a circle. Wrist kinematics were recorded and transformed to a right-hand polar coordinate system (left), in which the directions corresponding to flexion (flex), extension (ext), radial deviation (rad dev), and ulnar deviation (uln dev) are shown. The wrist kinematics was used to compute ECR tendon displacement and velocity, which were input into the six spindle models to predict Ia firing. The predicted firing rate profiles were compared to the recorded human ensemble data. The diagram above shows the experimental protocol for movement to target 6.

### ***3.2 Human Experiments***

Data used in this study was recorded during a previous investigation that used microneurography to record single unit activity in muscle spindle afferents during the centre-out task (Jones et al. 2001).

#### ***Centre-Out Task***

The centre-out task is a staple of sensorimotor neurophysiology and has been used extensively for 2D and 3D reaching experiments in monkeys and humans (Goodbody and Wolpert 1998; Schwartz et al. 1988; Scott and Kalaska 1997).

Our experiments of afferent responses during the centre-out task build on the wide spread use of these movements for studying sensorimotor systems.

The subject was seated in front of a monitor on which a cursor moved in relation to the subject's hand movement. The starting position is displayed by a central marker on the screen and corresponds to a neutral wrist position located at the centre of the circle seen in Figure 3.1, left. The subject was required to hold the cursor in this starting position until one of eight equally spaced targets around the circle was randomly lit and an audio cue signalled them to move the cursor to the target (Figure 3.1 shows numbering scheme of targets). Subjects were instructed to move accurately and quickly to the lit target. These movement velocities average 9 – 10 deg/s with peak velocities of 20 – 30 deg/s (Jones et al. 2001). Wrist kinematics and muscle spindle afferents were recorded during the performance of the task. There are three important phases of the task: *static hold-*

*centre* where the subject holds the cursor at the central marker, *dynamic move-to-target* phase where the subject moves the cursor quickly towards the target, and *static hold-target* phase where the target has been reached and the subject holds their wrist at that position. The separation between the static and dynamic phase becomes important when analyzing the afferent response characteristics.

### ***ECR Ia Recordings***

Eight ECR muscle spindle afferents were selected from a larger sample of data (Jones et al. 2001) to compare with the predicted firing rate of the spindle models. Once an afferent was identified as belonging to a muscle spindle, Ia's were identified based on their responses to tests designed to differentiate between primary and secondary afferents. A series of ramp-and-hold stretches were applied at different velocities; afferents that displayed a noticeable modulation of dynamic index were likely Ia's. Immediate bursting after a stretch following a static holding period was also indicative of a primary afferent. The subset of primary afferent data was selected because: the data was from putative Ia afferents in the ECR muscle; the responses were obtained during a centre-out task with predictable kinematics; and responses were obtained during movements to all eight targets. In a previous study of the ensemble response of spindle primary afferents in the cat hamstring, the authors reported that after five or six had been averaged to estimate a population response, the addition of more units did not change the population response significantly (Prochazka and Gorassini 1998b). On this precedent, we felt confident that our data sample was sufficient to

estimate general ensemble firing rate behaviour of human ECR spindle primary afferents.

### ***Ensemble Average***

The eight recorded ECR Ia afferent spike trains were aligned to movement onset and consolidated into one dataset. Since movement time to the target was not controlled for in these experiments, we recognize that there will be a resulting variability in our ensemble data due to these differing movement trajectories. An ensemble firing rate average was obtained by creating a spike histogram of this dataset with a bin width of 100ms. The histogram amplitude was divided by the bin width and the number of afferents in order to obtain the mean firing rate per bin. This served as the estimate for human ensemble ECR Ia instantaneous firing rate to which predicted firing rates from model simulations were compared.

### ***3.3 Model Simulations***

To generate predicted firing rates from the models that could be compared to the human ensemble data, we simulated the human centre-out movements, converted these movements to expected ECR tendon kinematics, and used this as input to the models. All movements and models were implemented and run in Matlab ver 7.0.4 and Simulink version 6.2. The specifics of each simulation step are now described.

### ***Centre-Out Task***

The centre-out wrist trajectories to each of the eight targets were defined in wrist-joint space and measured in degrees of joint rotation about the flexion/extension and radial/ulnar deviation axes. These trajectories were defined in two ways: (1) minimum jerk criteria is descriptive of target-directed wrist movements (Stein et al. 1988) and was used to simulate generalized movement to all targets and (2) the actual recorded kinematics from the eight subjects were averaged to give an ensemble trajectory to each target that was specific to our dataset. The amplitude of the minimum jerk movements was set to 7 degrees of joint rotation in order to match the ensemble movement amplitude. The three centre-out phases for the minimum jerk simulations were set to these time durations: hold-centre for 500ms, move-to-target for 650ms, hold-at-target for 500ms. The ensemble trajectories had a move-to-target phase of about 1s, with hold-centre and hold-target phases lasting at least 1s each. Model predictions in response to the minimum jerk trajectory were used in qualitative comparisons to real data from single units, while predicted firing rates in response to the ensemble trajectory were used to more accurately compare predicted and real ensemble firing rates both qualitatively and quantitatively.

### ***Tendon Displacement Model***

The rotations about the two axes of the wrist that describe the centre-out trajectories were used to calculate the tendon displacement of the ECR muscle resulting from the movements. These calculations were based on a human

cadaveric forearm study that reported equations for instantaneous moment arms with respect to joint rotation (Loren et al. 1996). The equation for tendon displacement (mm) in ECRb used in this thesis is:

$$x(t) = 16fem(t) + 0.08fem(t)^2 + 2.9 \times 10^{-4} fem(t)^3 - 1.45 \times 10^{-5} fem(t)^4 - 2.4 \times 10^{-7} fem(t)^5 - 16rud(t) + 1.06 \times 10^{-5} rud(t)^5$$

where  $x(t)$  is tendon displacement in mm

$fem(t)$  - wrist rotation in flexion/extension axis (flexion positive)

$rud(t)$  - wrist rotation in radial/ulnar deviation axis (radial positive)

Tendon displacement and velocity were then used as input to the six muscle spindle models. Corrections for compliance or muscle fibre pennation were not features of the spindle models tested, so were ignored for the present study.

### ***Ia Spindle Models***

Six muscle spindle models were used to generate predicted firing rate time series resulting from the simulated movements (Chen and Poppele 1978; Hasan 1983; Houk et al. 1981; Matthews and Stein 1969; Prochazka and Gorassini 1998a; b). All of these models were shown to have some predictive value for estimating ensemble Ia afferent firing rate during normal cat locomotion. The muscle spindle models were implemented in Simulink, using a previous published block-diagram (Figure 7 (Prochazka and Gorassini 1998b)). As the models were no longer available from the cited internet site, correct implementation was verified by comparing model behaviour to the published responses during cat locomotion (Figure 3 (Prochazka and Gorassini 1998b)). The solver used in our simulations

was the Euler algorithm with a time step of 1 ms. All model parameters were kept identical to the values of the parameters fitted to the previously reported cat locomotion data (Prochazka and Gorassini 1998b), with the exception of the baseline firing rate which was changed from 82 imp/s to 10 imp/s in order to be more reflective of our human data. The simulated predicted firing rates of the models should be interpreted as originating from hypothetical ECR muscle spindles, as all of our simulations were done in response to the presumed ECR tendon displacement during the centre-out task.

### ***3.4 Human and Model Data Comparison***

After simulation of the predicted model firing rates, comparison was made between each model and the ensemble data using the following measures: mean firing rate, directional tuning, static index, dynamic index, and temporal similarity. By consolidating all of these error measurements, a global error was computed for each model and the models were ranked in descending order of ability to predict human ensemble Ia firing rates.

#### ***Qualitative Comparison***

The human data was visually compared to the model data to look for general trends. Both ensemble and individual Ia afferents were analyzed to identify obvious differences between human data and model predictions. Differences between models during the different phases of the centre-out task (hold-centre, move-to-target, hold-target) were also identified.

### ***Mean Firing Rate***

Mean firing rates during the move-to-target (dynamic) and hold-target (static) phases of the centre-out task were calculated separately for both the ensemble data and model predictions. The squared difference between the human ensemble and individual model mean rate to each target were computed for both phases and summed over all eight targets. A final root mean square (RMS) mean firing rate error was calculated for each model by dividing the summed squared differences by the number of targets (eight) and taking the square root. The RMS mean firing rate errors were measured in impulses per second and were computed for all six models during both the move-to-target and hold-target phases of the centre-out task.

### ***Directional Tuning***

The most wide spread approach to analysis of neurophysiological data during the centre-out, or step-tracking, task is the ‘mean vector’ analysis method by which the directional tuning is determined (Gribble and Scott 2002). This approach has been extensively used for analysis of muscle spindle coding during passive movements of the ankle (Ribot-Ciscar et al. 2003) as well as a previous study of active and passive movements of the wrist (Jones et al. 2001). Briefly, for each target a vector was assigned with a length equal to the mean firing rate and angle set by the target angle. The resulting eight vectors, one for each target, were generated for the move-to-target phase (dynamic) and during the subsequent period of hold-target (static phase). The eight vectors were averaged to give a



mean vector. The angle of the vector is preferred direction and the normalized length is proportional to spread of tuning. For example, a length of 0 would result if the mean firing rate at each of the eight targets was the same, i.e. a uniform distribution of firing. Alternatively, if the mean firing rate was zero at all targets except one, the resulting mean vector length would be 1, i.e. perfect tuning. To test for significance of directional tuning, a bootstrap test was used where the mean rate and target angle are resampled from the original data (4000 resampling trials) and the resulting resampled vector length is compared to the original. If fewer than 200 resampled vectors are longer than the original, the directional tuning is considered significant with 95% confidence. Note, resampling is not done if the original mean vector length is less than 0.001, as this already indicates a non-directional distribution in circular statistics (Batschelet 1981).

A mean vector was computed for the human ensemble data and all of the model predictions for both the move-to-target and hold-target phases. There was no significant difference between the preferred directions (vector angle) of the models, and thus no error was computed for this measure. However, the spread of tuning (indicated by vector length) varied between models and thus the RMS error between model and human ensemble vector length was computed for each phase.

### ***Dynamic Index***

The Matthews' Dynamic Index is a widely used measure that captures the influence of changes in velocity on Ia firing rate by comparing neural responses to a ramp and hold stimulus (Jansen and Matthews 1962). Classically, the dynamic

index is calculated by taking the mean firing rate during the *latest* segment the ramp phase ( $f_{\text{peak}}$ ), and subtracting the mean firing rate during the hold phase ( $f_{\text{plateau}}$ ). As illustrated in Figure 3.2, this translates into the difference in firing rate when the muscle displacement is constant at its maximum stretch, but the velocity suddenly drops. Since the centre-out task follows a minimum jerk trajectory rather than ramp and hold, an altered version of the dynamic index was calculated for our experiments. In this ‘modified dynamic index’,  $f_{\text{peak}}$  was computed as the mean firing rate of a 100ms time window centered on peak velocity. Although peak velocity does not occur at maximum muscle stretch, if velocity is more dominant than displacement, this measure should still be reflective of a spindle afferent’s ‘dynamic’ response.

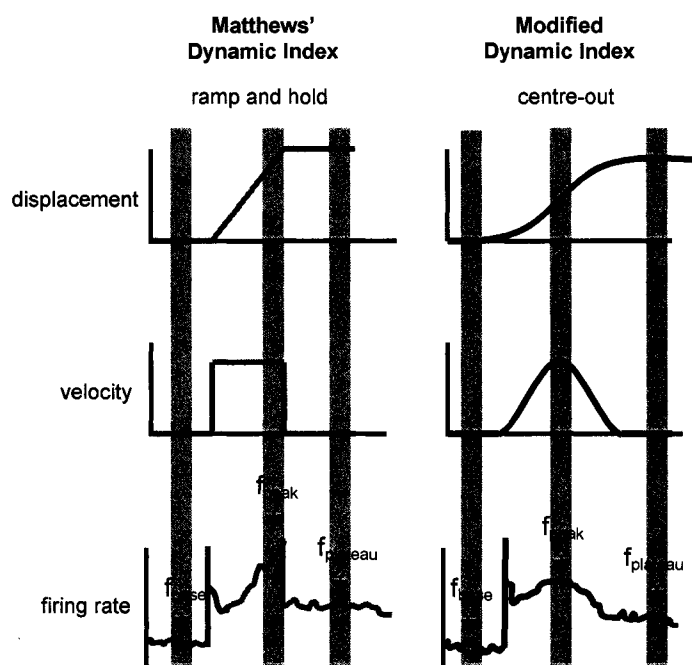


**Figure 3.2. Matthews' and Modified Dynamic Index.** Dynamic index =  $f_{\text{peak}} - f_{\text{plateau}}$ . The left column shows the classical way of finding the dynamic index parameters during a ramp and hold stimulus. The right column shows the modified dynamic index parameters used here. The calculation of  $f_{\text{peak}}$  occurs around maximal velocity during the centre-out task.

A dynamic index to each of the eight targets was calculated for the ensemble data and for each model. The squared difference of the dynamic index of individual models and the ensemble were summed over all targets. The final RMS dynamic index error for each model was computed by dividing the summed squared differences by the number of targets (eight) and taking the square root.

### ***Static Index***

The static index, defined as the mean firing rate at neutral position ( $f_{\text{base}}$ , Figure 3.2) subtracted from the mean firing rate at maximal displacement ( $f_{\text{plateau}}$ , Figure 3.2), was computed for the human ensemble data and all of the models to each target. Similarly to the dynamic index, the squared difference of the static index of individual models and the ensemble were summed over all targets. The final RMS static index error for each model was computed by dividing the summed squared differences by the number of targets (eight) and taking the square root.

### ***Temporal Similarity***

To evaluate the fidelity of model predictions to the ensemble data over all time, the difference between model and ensemble *instantaneous* firing rates were computed. The time series was divided into bins of 100ms width, and the squared difference in firing rate of the ensemble and individual models was computed for each bin, and summed over all bins and all targets. The final RMS instantaneous firing rate error for each model was computed by dividing the sum of squared

differences by the number of bins and number of targets, and taking the square root.

### ***Overall Model Ranking***

An overall error score was computed that takes all calculated errors into consideration and weights them equally. The overall error score was computed as follows. RMS errors from each measure (mean firing rate, directional tuning, dynamic index, static index, temporal similarity) were normalized by the median of the model errors of that measure. This normalized quantity is what we call a 'category error score'. The closer to zero that the 'category error score' is, the better the model is at estimating the human ensemble data for that category. The three models that have a performance value less than one are the best predictors of that particular measure. The category error score of each model is summed over all categories resulting in the 'overall error score'. This error score is not absolute, but rather a relative measure of the models against each other. The model with the lowest error score performs the best in predicting the human ensemble Ia firing activity *relative* to the other models.

## Chapter 4. Results

---

In this section we assess whether a group of six muscle spindle models, which have been developed and used to interpret data from cat studies, give a general and accurate prediction of the responses of human muscle spindles during a centre-out task.

### *4.1 Qualitative Comparison*

Here the general trend of responses in human spindle afferents and model spindles are compared during each phase of the centre-out movement (hold-centre, move-to-target, hold-target). This visual comparison gives valuable first insight into how the models behave during static (hold) and dynamic (move) phases of the task.

#### *Separation of static and dynamic phases in firing rate response to centre-out task*

Figure 4.1 shows the response of a single human spindle to two opposing targets, as compared to the predicted results of the six models during stereotyped minimum jerk movements to the same targets. Movement to target 2 corresponds to ECR muscle shortening and as can be seen in Figure 4.1, this muscle spindle was temporarily unloaded at the beginning of the movement phase resulting in a pause in the spike train (Figure 4.1, left upper trace). The corresponding estimated instantaneous firing rate trace (Figure 4.1, left middle trace), shows a transient period of decreased firing rate during movement followed by recovery of firing

rate during the static hold-target phase. Movement in the opposite direction to target 6 (ECR muscle stretch) resulted in a burst of action potentials with instantaneous firing rates reaching almost 90 imp/s, followed by adaptation to a lower rate during the static hold-target phase. The continuous firing rate estimate (smoothed using a 300ms Gaussian kernel) shows a clear separation of dynamic and static firing rate responses during ‘movement to’ and subsequent ‘holding at’ the target.

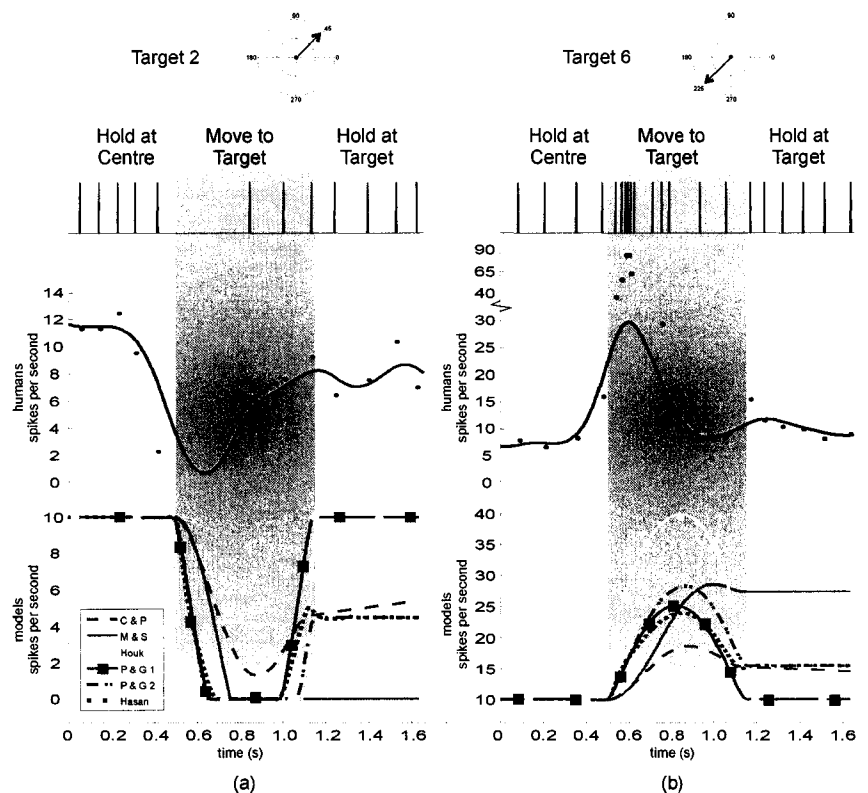


**Figure 4.1. Comparing movements to opposite targets.** Movement to target 2 as in (a) results in ECR muscle shortening, while movement to target 6 as in (b) results in ECR lengthening. Upper traces show the associated spike trains recorded from a single human ECR spindle during these movements. Middle traces show an estimate of the instantaneous firing rate (smooth line) overlaid on the actual recorded spike occurrences (dots). The smoothed estimate was obtained from the spike trains using a 300ms wide Gaussian kernel. Bottom traces show the six spindle model predictions of instantaneous firing rate in response to a simulated minimum jerk movement. The grey band indicates the movement time as simulated in the minimum jerk trajectory.

### ***Individual Ia afferent response versus model predictions with minimum-jerk trajectory***

The main interest of Figure 4.1 is in the comparison of the model predictions (Figure 4.1, coloured lines, bottom trace) with the single human Ia recordings. In this case the model predictions were generated by *approximated* movement characterized by a minimum-jerk trajectory. The changes in firing rate predicted by some of the models during movements to these same targets had similar dynamic and static phases. To target 2, all of the models showed a transient decrease in firing rate during the movement phase that is comparable to what is seen in the human. However, only three of the models (red, blue, purple) showed a recovery of firing rate during the static hold-target phase that was similar to what is seen in the humans: less than the hold-centre rate but higher than the minimum rate reached during the movement phase. Similarly for movement to target 6 all models showed a transient increase in predicted firing rate that was higher than the rate after reaching the target, but the blue, purple, and red models seem to match the relative difference in the human static hold-target phase rate the best. From these results it appears that even with an approximated minimum-jerk movement trajectory, three out of the six models are able to predict qualitative response characteristics quite well.

### ***Individual Ia afferent response versus model predictions with actual trajectory***

We now move on to looking at model predictions found by using the actual trajectory recorded from the human subjects during the centre-out task, rather than

the minimum jerk trajectory to simulate centre-out movement. This should give us a more precise representation of the models in comparison to human spindles.

A single ECR spindle was recorded during four repeated movements to target 7 (corresponding to pure ulnar deviation). In Figure 4.2, the first 1.5 seconds correspond to holding at center, movement to target comprises the following  $662 \pm 92$ ms, and the remaining time the subject is holding at the target. Model predictions in response to the averaged kinematics were simulated and are shown in the top trace of Figure 4.2. These model firing rates can be compared to the bottom trace which shows a histogram of the actual recorded instantaneous firing rate during the four trials. The human spindle has an average firing rate of 9 imp/s during the hold-center phase, reach a transient peak firing rate of 23 imp/s during movement, and settles to 12 imp/s during the static hold-target phase. The yellow model appears to be hypersensitive to the kinematics, under-predicting firing rate during the majority of the static phases (hold-center, hold-target) and over-predicting firing rate during the movement phase. Since the yellow model is so mismatched from the human data it will no longer be shown in temporal plots as it is distracts attention from the rest of the models. The orange model also clearly deviates from the general temporal pattern displayed by the human data since it barely reduces its firing rate once the static hold-target phase is reached, settling to 18 imp/s. The remaining models (red, green, blue, purple) follow the general temporal trend of the human data, although they all fall short of predicting the peak firing rate during movement to varying degrees. This indicates that



although the static sensitivities of these models and the human data seem to match, the dynamic sensitivities are slightly under-represented in the models.

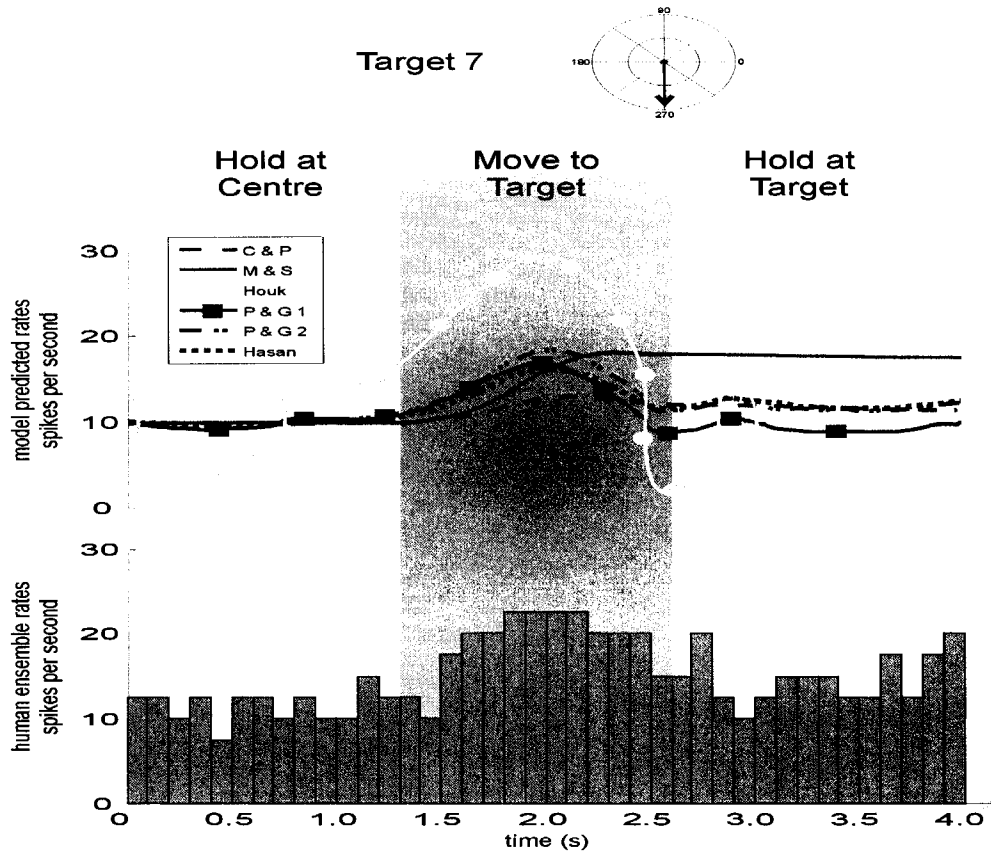


**Figure 4.2. Comparing multiple movements to the same target.** The bottom traces shows the histogram representation (bin width 100ms) of the average firing rate response recorded from a single human ECR spindle during four repeated movements to target 7. The kinematics during these movements were also recorded and averaged. The average movement duration of the four trials is  $662 \pm 92$ ms (mean, sd), with movement onset occurring at 1.5 seconds. The top trace shows the predicted firing rates from the six models in response to the same movement.

### ***Ensemble Ia afferent response versus model predictions with actual trajectory***

Since the models were originally fit to ensemble cat data, it is most instructive to compare the model responses to ensemble human data. Figure 4.3 shows this comparison with an ensemble that includes eight human ECR spindles. The bottom traces are the histogram-estimated ensemble firing rate to target 2 (ECR

shortening) and target 6 (ECR lengthening). The movement phase of the ensemble is between 0.5 and 1.5 seconds and is marked by the shaded grey area. The top traces are the predicted firing rates of five models in response to the ensemble kinematics. The orange model is once again doing a poor job of predicting the general human spindle temporal dynamics due to its underestimation of hold-target firing rate for target 2, and overestimation for target 6. During the dynamic movement phase to target 2, the blue, green, and purple models all either significantly reduce firing or go completely silent. This is unlike the human ensemble result, which transiently reduces firing rate but never completely shuts off. Only the red model is consistent with this result. During the dynamic phase to target 6 the blue, green, purple, and red models all predict a transient increase in firing that is consistent with the trend seen in the ensemble, but with varying peak rates reached. The quantitative analysis in later sections will serve as a more complete measure to rank these remaining four models in terms of their ability to predict human spindle firing. For now what is important to remark is that a given model's predictive ability varies depending on the location of target and phase of movement. It is also important to note that none of the models predict the almost *immediate* decrease/increase of firing rate exhibited by the human ensemble upon movement onset. It appears that only the underlying slower temporal dynamics are represented in the models.

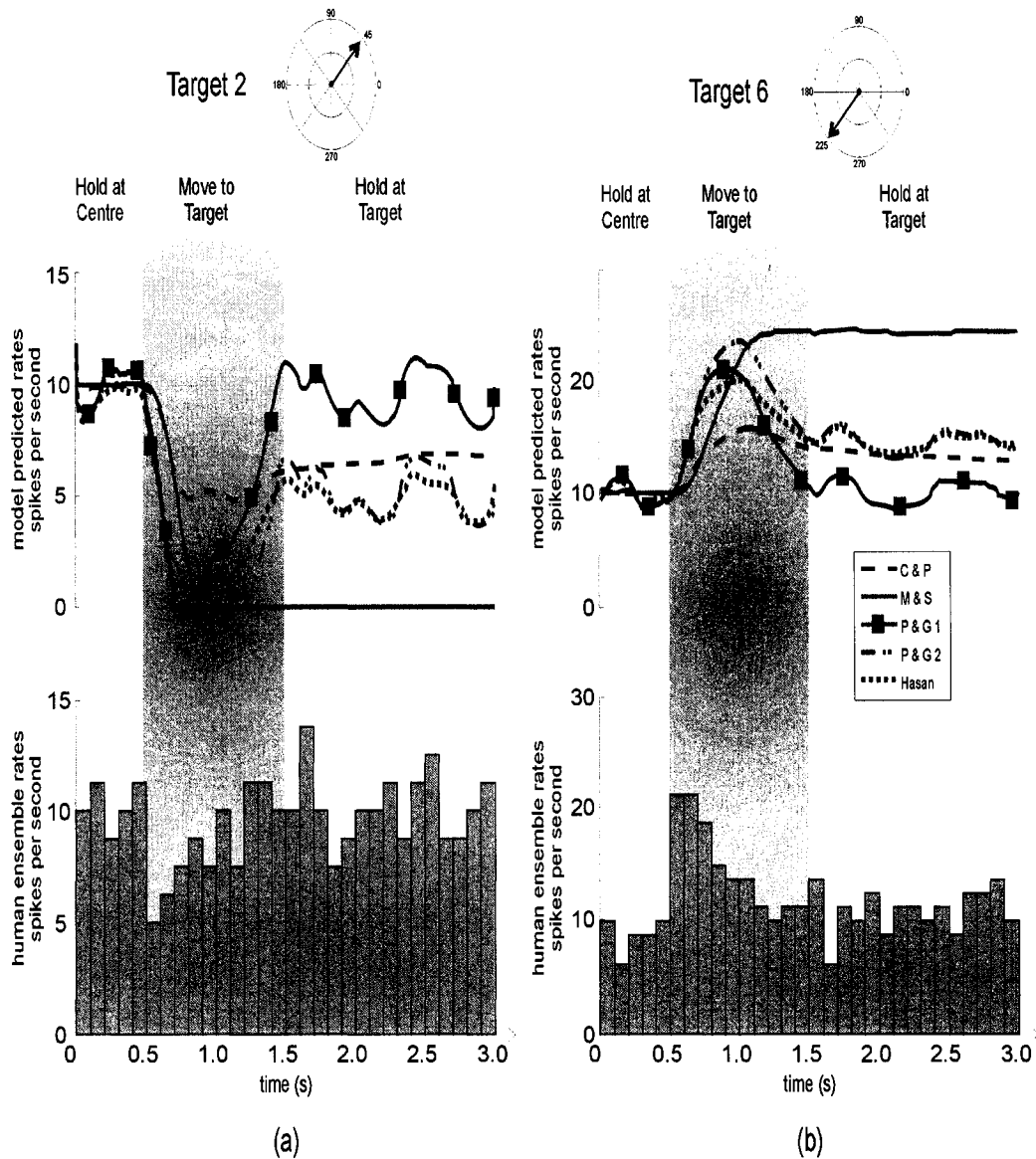


**Figure 4.3. Comparing models and human ensemble data to two opposing targets.** Eight human spindles from the ECR muscle were recorded during the centre-out task. This data was averaged to generate human ensemble firing rates and kinematics. a) Movement to target 2 corresponds to ECR muscle shortening (tendon displacement and velocity top two traces). Five model predictions in response to ensemble wrist kinematics to target 2 (middle trace) and histogram with bin width of 100ms representing ensemble firing rates (bottom trace) during movement to target 2. b) Movement to target 6 corresponds to ECR muscle lengthening (tendon displacement and velocity top two traces). Five model predictions (middle trace) and histogram with bin width of ensemble firing rates (bottom trace). General temporal dynamics of the human data is captured by the red, green, blue and purple models. However, it is the slower temporal dynamics that is represented in the models, as the immediate human ensemble firing rate drop (a) or increase (b) aligned with movement onset (at 0.5 seconds) is not found in the model predictions.

### ***Overall model impressions from qualitative comparison to human data***

From the qualitative comparisons of the model predictions to both single unit and ensemble activity, it has become obvious that some models predict human spindle activity better than others. The yellow and orange models are unable to capture the general temporal characteristics seen in the human data during the centre-out task. The yellow model is overly sensitive in all phases of the task, while the orange model is overly length sensitive which results in an over-prediction of firing rate during static stretches, and an under-prediction during static shortening. The remaining four models differ the most in their sensitivity during the transient dynamic (move to target phase) with the exception of the green model which has no static sensitivity component and therefore does not distinguish between the two static phases (hold-center and hold-target). However, although the human data does show a slight difference in firing rate between these two static phases, it is a minimal enough difference that it does not warrant excluding the green model just based on qualitative comparisons.

### ***4.2 Mean Firing Rate***

Differences in mean firing rate during the move-to-target phase and hold-target phases were computed between the ensemble human data and the six model predictions. Figure 4.5a shows a summary of the RMS mean firing rate errors for each model during both task phases. The red, blue, and purple models had the most accurate predictions, with errors less than 3.5 imp/s during both phases. All three of these models were closer in their mean firing rate estimates during the

static hold-target phase of the task. This suggests that dynamic movement is not as well represented by the models. As already suggested by qualitative analysis of Figure 4.3, these three models have the potential to capture the slow temporal dynamics of the human ensemble data during the movement phase, but a possible point of improvement could come in more precisely capturing the fast response at onset of movement seen by a burst of action potentials or sudden drop in firing rate.

The yellow and orange models do a poor job in predicting mean firing rate for both phases. The green model however predicts an RMS error of less than 3 imp/s during the movement phase of the task, but loses its predictive ability in the static hold-at-target phase where its RMS error grows to over 9 imp/s (Figure 4.5a). The green model is strictly velocity dependent, and thus during the static hold-target phase predicts a firing rate equivalent to the background firing rate when the wrist is in neutral position. This is inconsistent with the human ensemble data which appears to be both velocity and length dependent.

### ***4.3 Directional Tuning***

Human muscle spindles have been characterized by their preferred direction in the past. In this section we report the directional tuning of the human ensemble in comparison with the tuning of the model predictions. Directional tuning was assessed for both the dynamic ‘move-to-target’ phase of the centre-out task, and the static ‘hold-target’ phase. Mean vectors were computed from the mean rates to each target during both the dynamic and static phases as outlined in the

Methods section. The angle of the mean vector is the preferred direction, and the normalized length of the vector is an indication of sharpness of tuning (0 is not tuned, 1 is perfectly tuned).

Directional tuning was computed for individual afferents as well as the ensemble. Six of the eight afferents were found to be directionally tuned during the dynamic (move) phase (bootstrap,  $p < 0.05$ ) while only three were significantly tuned during the static (hold) phase. The data was then used to estimate the directional tuning for the population. The mean vector for the dynamic phase had a normalized length of 0.28 and an angle of 239 degrees. The mean vector for the static phase was 0.11 long with an angle of 240 degrees. A bootstrap test showed that both vectors were significantly tuned ( $p < 0.05$ ). This result differs from the previous study in which these units were part of a larger sample of ECR spindle afferents. In the previous study, the data were not significantly tuned during the static phase (Jones et al. 2001).

All the models showed directional tuning during the dynamic phase with a mean vector angle of approximately 215 degrees. The lengths of the mean vectors are given in the legend for Figure 4.4 where the directional tuning is illustrated in polar coordinates. The grey band illustrates 95% confidence interval of the distribution of the human ensemble data and the black arrow indicates the direction of the mean vector. The accuracy of the mean vector angle predicted by the models (Figure 4.4, red arrow) was surprising given the variability in the human data and the simplifying assumptions for the biomechanical wrist model and simulations. The human data shows higher firing rates than those predicted by

the models in the direction opposite the preferred direction, which could be due to co-activation of gamma or beta motor neurons not accounted for in these simulations.

To quantify the differences in tuning spread between the ensemble data and the predicted models, RMS errors of the normal vector lengths were calculated. Figure 4.5b summarizes these results. Overall the red, green, blue, and purple models have the least tuning spread error for both the move-to-target and hold-target phases. However, these results must be interpreted with caution because the green model is not directionally tuned during the static hold-target phase while the other three models are tuned. The appropriate model largely depends on the spindle in question because as previously outlined, both scenarios are present in the human population.

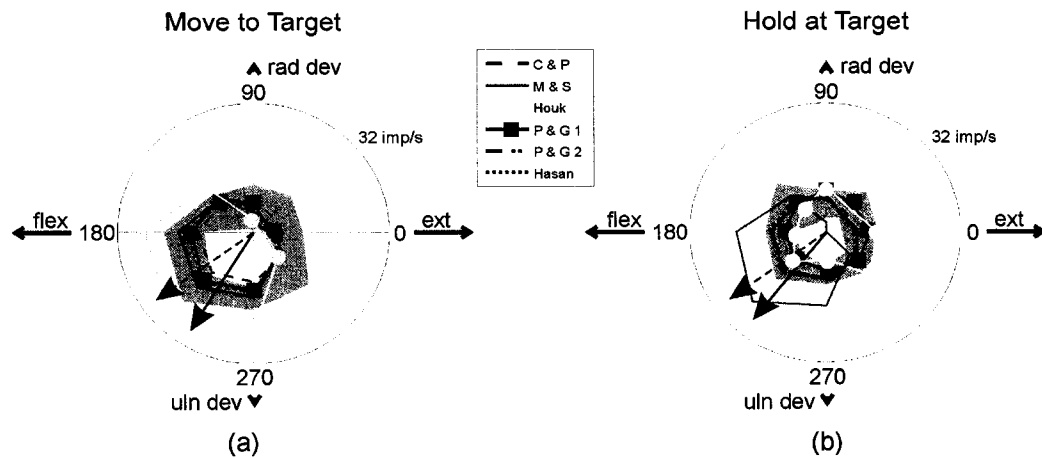


**Figure 4.4. Comparing directional tuning in polar plots.** (a) Mean firing rate for the models (see legend) and 95% confidence interval of averaged human data (grey area) are shown to each target. The preferred direction of the models (computed by mean vector) was 215 degrees (red arrow) and the preferred direction of the human data was 239 degrees (black arrow). The length of the normalized mean vectors (not illustrated) were: 0.28 (human), 0.20 (red), 0.46 (orange), 0.54 (yellow), 0.30 (green), 0.42 (blue), 0.34 (purple). (b) Mean firing rates during the static phase of holding on each target. Two models (yellow and green) were not significantly tuned during the hold phase, while the others had the same preferred direction (215 deg) and normalized mean vector lengths of: 0.16 (red), 0.60 (orange), 0.22 (blue), 0.22 (purple). The mean vector for the human data had an angle of 240 deg and a length of 0.11, which was significant ( $p < 0.05$ ).

#### 4.4 Static Index

The static index is a measure of the sensitivity of spindle afferents to changes in muscle length. The index is defined as the difference between  $f_{\text{plateau}}$  and  $f_{\text{base}}$  and in our experiment measures the firing rate change in ECR Ia afferents when the wrist moves from the neutral central position to the target position. The RMS error in predicted static index of each model is illustrated by the hatched bars in Figure 4.5c. The red, blue, and purple models predict the most accurate static index, all with RMS error less than 2 imp/s. All of these three models show a relatively equal performance in this category.



## 4.5 *Dynamic Index*

The dynamic index was calculated for each model and the ensemble human data as the difference between  $f_{\text{peak}}$  and  $f_{\text{plateau}}$  as illustrated in Figure 3.2. The RMS error in dynamic index for each model is compared in Figure 4.5c, solid bars. The only model that seems to do a reasonable job at predicting the correct dynamic index is the red model with an error of 3 imp/s. All of the other models over-predict the dynamic index by at least 4.7 imp/s, with the exception of the orange model which under-predicts the dynamic index by 5.5 imp/s.

Since  $f_{\text{peak}}$  was measured at the peak velocity of movement which comes *after* movement onset, the fast change in firing rate such as ‘bursting’ or transient ‘silencing’ seen in the ensemble human data is not reflected in this measure. Rather, the slower temporal dynamics in response to movement are captured. Taking this into consideration, it appears that the best predictor of the slow adaptation of muscle spindle afferents is the red model, while all other models (excluding the orange model) seem to place too much emphasis on velocity dependence. The error in the orange model arises from the opposite problem – too little sensitivity to velocity results in negligible change between  $f_{\text{peak}}$  and  $f_{\text{plateau}}$ .

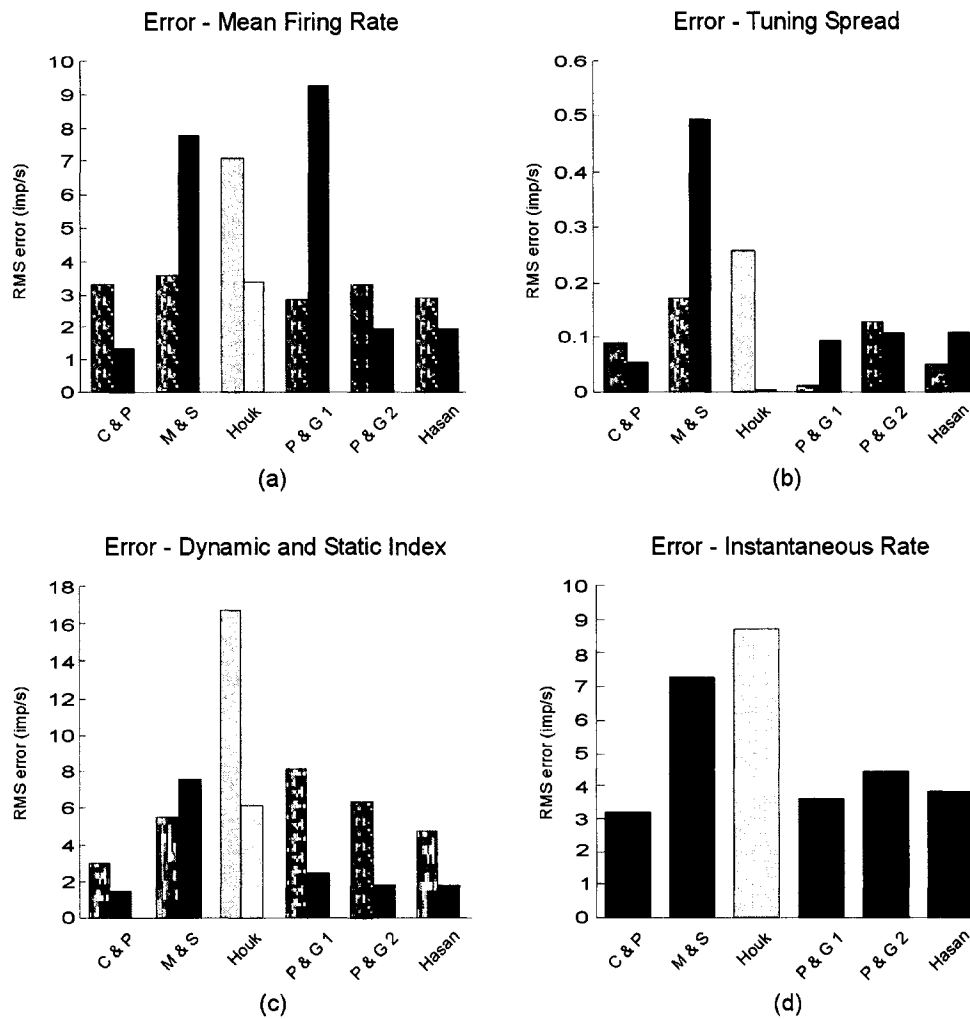


**Figure 4.5. Comparing model errors for different error categories.** (a) RMS error in mean firing rate during move-to-target (hatched) and hold-at-target (solid) phases of centre-out task. (b) RMS error in normalized mean vector length for each model. Vector length is directly related to the tuning spread of the spindle afferent and thus error in length can be interpreted as error in tuning spread. Hatched bars are during the move-to-target phase, solid bars are during the hold-at-target phase. (c) RMS errors in dynamic (hatched) and static (solid) indices. (d) RMS error in instantaneous firing rate of each model. This was computed over the whole time series of the task and is reflective of each models' temporal similarity to the ensemble data.

#### 4.6 Temporal Similarity

Models were assessed on their ability to predict human ensemble data at all time points during the task. This measure is essentially equivalent to the average RMS error in instantaneous firing rate for each model. Figure 4.5d compares the

overall errors of all models. The red, green, and purple models have the smallest errors, ranging between 3 and 4 imp/s.

#### 4.7 Overall Model Ranking

In order to come up with an overall ranking of models in terms of predictability of human ensemble Ia afferent activity, all quantitative errors including mean rate, tuning spread, dynamic index, static index, and temporal similarity were combined into one global error measurement. RMS errors were normalized by dividing by the median model error in each category. These normalized errors were then summed over all categories resulting in a total normalized error for each model (Table 4.1). Although there is no upward cap on this error (no limit to inaccuracy), the bottom limit is a score of zero, which corresponds to perfect predictive ability of the model.

	Mean Rate		Directional Tuning		Dynamic Index	Static Index	Temporal Similarity	TOTAL ERROR
	Move	Hold	Move	Hold				
<b>Chen&amp;Poppele</b>	1.0	0.5	0.8	0.5	0.5	0.7	0.8	<b>4.8</b>
<b>Matthews&amp;Stein</b>	1.1	2.9	1.6	4.8	0.9	3.5	1.8	16.6
<b>Houk&amp;etal</b>	2.1	1.3	2.4	0.1	2.8	2.9	2.1	13.6
<b>P&amp;G1</b>	0.9	3.4	0.1	0.9	1.4	1.2	0.9	8.7
<b>P&amp;G2</b>	1.0	0.7	1.2	1.1	1.1	0.8	1.1	7.0
<b>Hasan</b>	0.9	0.7	0.5	1.1	0.8	0.8	0.9	5.8

**Table 4.1. Normalized model errors.** RMS errors were normalized by dividing by the median error of the six models in each category. Any normalized errors less than one indicates the model is in the top three in predictive ability for that category. The last column is a sum of the normalized errors for each model. The red model (Chen & Poppele) has the lowest summed error and thus is considered the best predicting model of our ensemble human data.

The red model has the least total error with a score of 4.8. The purple and blue models also have relatively low error scores of 5.8 and 7.0 respectively.

Therefore from a global error perspective the red, purple and blue models tend to generalize best from cat locomotion data to our human ensemble data by producing the least amount of relative error in their predictions of five different descriptors of muscle spindle Ia afferent activity.

## Chapter 5. Discussion and Conclusion

---

### 5.1 Discussion

Muscle spindles are an important source of sensory feedback that signal information to the central nervous system about movement around joints (Gandevia 1996; Prochazka 1996; Stein et al. 2004). Recordings from muscle spindle afferents can be difficult, especially in behaving animals. Nonetheless single afferents have been recorded in cats, monkeys and humans, although the experimental yield is usually low. As an attempt for further understanding of spindle responses, mathematical models have been derived based on the data from one of the most studied species: cats. If these models represent spindle afferents well, they could be useful in probing primary afferent feedback in the absence of large datasets, in analysis of hypothetical responses to untested movements, and could be incorporated into closed-loop neural prosthetic systems. However, before solid faith can be put into the existing models, they must be validated against a wide variety of spindle recordings. There has been no validation against a human dataset until now. In simulations of centre-out movements, we found that the ensemble firing rate and directional tuning of human ECR afferents (presumably Ia) was adequately captured by three of the six models: Chen & Poppele (red), Hasan (purple), and Prochazka & Gorassini 2 (P&G2, blue). Our results indicate that the red (Chen & Poppele) model has the best overall

predictive ability. This is consistent with the findings of the models best fitting models to cat locomotion data (Prochazka and Gorassini 1998b).

In the rest of this discussion, the strengths and weaknesses of the models will be addressed with respect to length and velocity sensitivity, temporal dynamics, and their ability to predict single and ensemble human data. The lower background firing rate seen in human primary afferents in comparison with cats is also discussed, and our results are used to speculate whether fusimotor drive is involved in this discrepancy. Finally, limitations of our study are outlined to reiterate the context under which our results should be interpreted.

### ***Finely-tuned length and velocity sensitivity***

The main divergence between the top three models (red, purple, blue) and the bottom three (green, yellow, orange) is in their ability to predict firing rates during the static (hold-target) phase of the task. The green model (Prochazka & Gorassini 1) had absolutely no length sensitivity built-in, and thus a static lengthened or shortened muscle would elicit the same response. This ambiguity is not seen in the human spindle primary afferents. The yellow model (Houk et. al) takes into account both length and velocity components of movement; however with the parameters chosen to fit the cat locomotion data, the representation of velocity overpowers that of length in response output at the tested human velocities. This leads to the yellow model showing virtually no length sensitivity for the range of human data. The orange model (Matthews & Stein) did poorly in

the model evaluations for the opposite reason as the green and yellow models; there was too much length sensitivity.

It should be noted that the maximum velocity for the cat data ranged from 148 to 205mm/s, whereas our human data maximal velocities were much lower at 5 mm/s. Ignoring fusimotor influence for now, if it is assumed that muscle spindles do not change mechanical properties during movement, a good model should be able to fit movement at all physiologically relevant speeds equally well without changing parameters. One of the impressions from the literature is that movements during human studies are inevitably restricted in range and velocity to permit stable percutaneous recordings, and are thus *not* physiologically relevant. Given that the 5 micron tip of a microelectrode must remain in intimate relationship with an axon of about 10 microns in diameter while movements are being made in the same limb, this suspicion is not unwarranted. However, during the centre-out task from this study subjects were instructed to move accurately and quickly and there were no explicit instructions to move slowly to prevent dislodging the microelectrode from the nerve. Thus the results from movements at these velocities are 'natural' during directed movement, and should not be dismissed. The shortcomings of the green, yellow, and orange models appear to be in their balancing of velocity and length components; when the models are fitted to work well for one velocity range they fail for another. In Prochazka and Gorassini's study of the models fitted to cat locomotion data, the green model actually faired quite well, despite its complete absence of a length component (Prochazka and Gorassini 1998b). It is not unexpected that velocity would be the

dominant component in high-speed movements, but the eloquence of the successful models comes from the appropriate reflection of length and velocity components in more than one velocity range.

Further investigations need to be done in order to ensure robustness of these models under all movement speeds and displacements. The most rigorous way to test for the contribution of length and velocity would be to impose a movement task in which these components are independent or de-coupled. Both in locomotion and directed movements, position and velocity profiles of limb kinematics are highly stereotyped; by knowing one of the profiles the other can usually be deduced (Stein et al. 1988). Future microneurographic experiments could be geared towards a random-pursuit tracking task in which movements would be geared toward following a randomly moving cursor that is statistically matched to move in the space that fit the ergonomics of the limb in question. For example, statistics of published ergonomics of the wrist (Serina et al. 1999) could be used as the basis for the position and speeds that the cursor will move, but these positions and speeds will be introduced randomly such that no interdependence results in the kinematics. This will ensure that the spindle afferents are being exposed to the statistics of stimuli normally encountered in natural movement, while avoiding the undesirable coupling of position and velocity. This type of dataset would pose a significant challenge for the models to perform well in a large unconstrained physiological range. The model that succeeds in conquering such a dataset could be looked upon with confidence.



### ***Slower temporal dynamics dominate the models***

Immediately after the onset of a movement, individual human spindle primary afferents often show a transient burst or drop in activity; burst for stretch, drop for shortening. Bursting is often smeared to some extent in ensemble data because the rate and time course is different in individual spindles. However, given our small sample size of only eight afferents, this very quick change in rate from baseline firing can still be seen in our data in Figure 4.3. We will call this phenomenon the ‘fast temporal dynamics’ of afferent activity. A much more gradual change in firing rate occurs after primary afferents recover from the initial burst or drop in activity. This is evident in our centre-out task, where after the immediate drastic increase or decrease in firing rate of about 7-10 imp/s within 100ms at the onset of the move-to-target phase, the change becomes more continuous with firing rate changing in increments of 2-3 imp/s per 100ms as the movement continues. This more gradual change we will refer to as ‘slow temporal dynamics’ of afferent activity. The fast dynamics are most noticeable at the onset of movement, and are not very well captured by any of the models (Figure 4.3). Instead, the models seem to capture the underlying slow dynamics of the changes in firing rate, with the three top models showing a similar distinct separation between the hold-centre, move-to-target, and hold-target phases as seen in the human data.

### ***Single unit vs. ensemble responses***

The inability of any of the models to predict fast dynamic bursts or drops in activity is not a worrisome shortcoming if it is ensemble data that is of principal interest. Ensemble data often has the effect of smearing bursting patterns away through averaging. Should single units be of interest though, the purple (Hasan) model can be used since it has the built-in ability to mimic bursting with a change in parameter  $p$ . However, representing individual primary afferents with the blue (Prochazka & Gorassini 2) model will fall short in predicting fast dynamics.

Another area where single units may behave differently from the ensemble is in their directional tuning. When the directional tuning of the eight recorded muscle spindle afferents were compared to the models on an individual basis, four of the human spindles responded similar to the blue and purple models (directionally tuned for movement & hold phase), three had responses like the green model (directionally tuned only during movement) and the remaining unit was unlike any of the models. So while on average, the human data is directionally tuned in the static phase, on an individual basis some units behave as if they are only sensitive to velocity as in the green model. From this finding we can infer that more than one model may be required to capture the encoding properties of individual human muscle spindle primary afferents.

### ***Lower background firing rate in humans – difference in static motor drive?***

The contentious issue of why there has continually been a lower background firing rate recorded in human primary afferents than in cats has been

acknowledged rather than addressed in this study. The discrepancy in rates is usually 50 to 110 imp/s, and is speculated to arise from a high level of tonic gamma static motor neuron activity in cat experiments (Prochazka and Gorassini 1998a; b). Tonic gamma static drive would result in an increased *offset* or *bias* which could explain the background difference. To get around this in our study, we simply subtracted an offset of 72 imp/s from the output of the models, bringing the background firing rate down to be more at par with our human data. Our results show that just with this simple subtraction of an offset, three of the cat models can adequately predict human firing rates. Since all other parameters were kept the same and the models predicted fairly well during the movement phase of the centre-out task, it is unlikely that the *dynamic* gamma motor drive changes significantly across species for the tasks that these models were based on. This supports the hypothesis that there exists increased tonic gamma *static* drive in cats but does not explain it. The reasoning behind the possible difference in CNS static motor control in cats and humans needs to be further elucidated. Perhaps it is a difference in central processing rather than muscle spindle physiology that has led to this discrepancy. Or perhaps the differences in tasks and the experimental environments were the cause. More controlled experiments in humans are necessary to make further speculations. It has been shown that both static and dynamic fusimotor drive is highly task-dependent within cats (Kandel et al. 2000). It would be interesting to see what kind of tasks change the dynamic and static drives in humans, and how this relates to similar tasks in cats.

Subtraction of a bias to achieve a lower background firing rates in the models also had the effect of predicting considerable periods of silence during simulated movements that match the centre-out task. Although our human data shows some evidence of afferent silencing, the majority of our ensemble data maintains some background firing irrespective of the corresponding movement. Therefore the periods of zero firing rates predicted by the models is questionable and should be further explored in human experiments. This also suggests that if the human spindles do somehow compensate to avoid silent periods, a simple decrease in static gamma drive may not be the only effect behind the difference in background firing rates. A zero-saturation signal would introduce ambiguous results for both central nervous processing and if implemented in a biomimetic control system.

### ***Rate versus temporal coding***

One of the assumptions underlying all the models used in this study is that the important unit for coding in muscle spindle primary afferents is rate; after all the output of all of the models is instantaneous firing rate. This assumption implies that the nervous system, in its decoding process, is not interested in the actual timing of individual spikes, but rather is concerned with an average measure of rate to deduce muscle position. This indeed seems plausible since we have shown that to a degree, length and velocity can indeed predict rate; therefore rate must be informative of muscle state. Moreover, spindle afferents are directionally tuned by mean firing rate during both static and dynamic phases of the centre-out task. However, the existence of the relationships between firing rate and direction,

length, and velocity, does not necessitate this rate decoding scheme in the nervous system. A common phenomenon in our data that was not captured by any of the models was bursting at the onset of movement. Even after averaging the eight afferents, a sudden increase or decrease in ensemble firing rate for lengthening and shortening movements after a static-hold phase can markedly be seen.

Perhaps in these short instances, when rate is not proportional to a physical measure, the timing of the spikes in the burst becomes more important. This hypothesis has recently been tested on the response of sensory neurons in the fingertip. Johansson and Birznieks show a correspondence between first-spike latencies after force stimulation to the finger tip, and direction of applied force (Johansson and Birznieks 2004). Their study provided evidence that relative timing of spikes from individual afferents contains information about object shape and force direction. This temporal coding scheme is also more congruent than rate coding with the fast behavioural responses that can be elicited to tactile stimuli (Johansson and Birznieks 2004). A similar study has not yet been performed on muscle spindle afferents, and it would be interesting to see whether similar findings would emerge.

### ***Limitations of the study***

Our emphasis was on a *first order* assessment of the applicability of these models for developing control systems relevant to human neurorehabilitation. We therefore decided to apply the models using the same parameters that gave the best fit of the ensemble firing rate for nine hamstring spindle primary afferents

during normal locomotion in chronic cat experiments (Prochazka and Gorassini 1998b), *without* refitting them to the human data. As a consequence our results focus more on which model best generalizes from cats to humans rather than on which is better for one particular species. From the looks of it, the red, purple and blue models are the most universal. It should also be noted that the analysis in our study emphasizes the *relative* predictive abilities between models, rather than the *absolute* errors of the models. As such, no ‘tolerable’ error was defined since the importance was put on each model’s ability to generalize rather than to minimize error. Now that a ranking order has been established, a more refined study could be done by fitting the top three models to human data. This would be best left until a richer dataset than ours has been acquired; one with ample sampling of physiological muscle displacement and velocities would be ideal.

We have also neglected to include modulatory fusimotor terms in the models. Given that fusimotor activation is task dependent (Kandel et al. 2000), and that levels of static and dynamic drive may change during a task (Taylor et al. 2004), and that these activation levels have not been meticulously categorized, the usefulness of adding such terms is questionable at this point. However, there has been speculation of alpha-gamma coactivation, where fusimotor and alpha motor neurons are activated simultaneously. This would be the equivalent effect of activation of beta motor neurons. Since EMG is proportional to motor neuron activation, it has been suggested that adding a scaled EMG signal could mimic such coactivation (Prochazka and Gorassini 1998a; b).

Despite all the simplifications inherent to our study, as a first order approximation three of the models studied have clear predictive value for estimating human ECR muscle spindle response during wrist movements. With further refinement they have the potential to become a powerful tool to simulate feedback in our sensory system and give us better insight into our sense of proprioception.

## **5.2 Conclusion**

Our goal in this report was to compare six muscle spindle primary afferent models against human data to determine whether the cat models, with no changes in parameters, can generalize to humans. With a limited dataset we have shown that, to a first order approximation, cat and human muscle spindle primary afferents are quite similar. The models with the best ability to generalize between species are the red (Chen & Poppele), purple (Hasan), and blue (Prochazka and Gorassini 2). It must be emphasized that this study was the first attempt at evaluating these models at an inter-species level. More experimental data across species will therefore be useful in validating and fine-tuning the models even further in the future.

## References

---

- Batschelet E.** *Circular Statistics in Biology*. London: Academic Press, 1981.
- Boyd-Clark LC, Briggs CA, and Galea MP.** Muscle spindle distribution, morphology, and density in longus colli and multifidus muscles of the cervical spine. *Spine* 27: 694-701, 2002.
- Boyd I, Gladden, M.** Morphology of mammalian muscle spindles: review. In: *The Muscle Spindle*, edited by Boyd I, Gladden, M. New York: Stockton, 1985.
- Breit S, Schulz JB, and Benabid AL.** Deep brain stimulation. *Cell Tissue Res* 318: 275-288, 2004.
- Chen WJ, and Poppele RE.** Small-signal analysis of response of mammalian muscle spindles with fusimotor stimulation and a comparison with large-signal responses. *J Neurophysiol* 41: 15-27, 1978.
- Cohen H.** *Neuroscience for Rehabilitation*. Lippincott Williams & Wilkins, 1999.
- Cole J.** *Pride and a daily marathon*. MIT Press, 1995.
- Enderle JD, Blanchard, S.M., Bronzino, J.D.** *Introduction to Biomedical Engineering*. Toronto: Academic Press, 2000.
- Gandevia SC.** Kinesthesia: roles for afferent signals and motor commands. In: *Handbook of Physiology, section 12, Exercise: Regulation and Integration of Multiple Systems* edited by Rowell L, Shepherd, J.T. New York: American Physiological Society, Oxford University Press, 1996, p. 128-172.
- Gandevia SC, Hall LA, McCloskey DI, and Potter EK.** Proprioceptive sensation at the terminal joint of the middle finger. *J Physiol* 335: 507-517, 1983.
- Gandevia SC, and McCloskey DI.** Joint sense, muscle sense, and their combination as position sense, measured at the distal interphalangeal joint of the middle finger. *J Physiol* 260: 387-407, 1976.
- Goodbody SJ, and Wolpert DM.** Temporal and amplitude generalization in motor learning. *J Neurophysiol* 79: 1825-1838, 1998.
- Goodwin GM, McCloskey DI, and Matthews PB.** The contribution of muscle afferents to kinaesthesia shown by vibration induced illusions of movement and by the effects of paralysing joint afferents. *Brain* 95: 705-748, 1972a.
- Goodwin GM, McCloskey DI, and Matthews PB.** The persistence of appreciable kinesthesia after paralysing joint afferents but preserving muscle afferents. *Brain Res* 37: 326-329, 1972b.
- Gribble PL, and Scott SH.** Method for assessing directional characteristics of non-uniformly sampled neural activity. *J Neurosci Methods* 113: 187-197, 2002.
- Hasan Z.** A model of spindle afferent response to muscle stretch. *J Neurophysiol* 49: 989-1006, 1983.
- Houk JC, Rymer WZ, and Crago PE.** Dependence of dynamic response of spindle receptors on muscle length and velocity. *J Neurophysiol* 46: 143-166, 1981.
- Hunt CC.** Relation of function to diameter in afferent fibers of muscle nerves. *J Gen Physiol* 38: 117-131, 1954.



- Jansen JK, and Matthews PB.** The central control of the dynamic response of muscle spindle receptors. *J Physiol* 161: 357-378, 1962.
- Johansson RS, and Birznieks I.** First spikes in ensembles of human tactile afferents code complex spatial fingertip events. *Nat Neurosci* 7: 170-177, 2004.
- Jones KE, Wessberg J, and Vallbo AB.** Directional tuning of human forearm muscle afferents during voluntary wrist movements. *J Physiol* 536: 635-647, 2001.
- Kandel E, Schwartz JH, and Jessell TM.** *Principles of Neural Science*. New York: McGraw-Hill, 2000.
- Kokkorigiannis T.** Somatic and intramuscular distribution of muscle spindles and their relation to muscular angiotypes. *J Theor Biol* 229: 263-280, 2004.
- Loren GJ, Shoemaker SD, Burkholder TJ, Jacobson MD, Friden J, and Lieber RL.** Human wrist motors: biomechanical design and application to tendon transfers. *J Biomech* 29: 331-342, 1996.
- Lyons GM, Sinkjaer T, Burridge JH, and Wilcox DJ.** A review of portable FES-based neural orthoses for the correction of drop foot. *IEEE Trans Neural Syst Rehabil Eng* 10: 260-279, 2002.
- Matthews PB, and Stein RB.** The sensitivity of muscle spindle afferents to small sinusoidal changes of length. *J Physiol* 200: 723-743, 1969.
- Matthews PBC.** *Mammalian muscle receptors and their central actions*. London: Edward Arnold Publishers 1972.
- McCloskey DI.** Muscle, cutaneous and joint receptors in kinaesthesia. In: *Neural control of movement*, edited by Ferrell WR, Proske, U. New York: Plenum Press, 1995.
- Peck D, Buxton DF, and Nitz A.** A comparison of spindle concentrations in large and small muscles acting in parallel combinations. *J Morphol* 180: 243-252, 1984.
- Prochazka A.** Proprioceptive feedback and movement regulation. In: *Handbook of Physiology, section 12, Exercise: Regulation and integration of multiple systems*, edited by Rowell L, Shepherd, J.T. New York: American Physiological Society, Oxford University Press, 1996, p. 89-127.
- Prochazka A, and Gorassini M.** Ensemble firing of muscle afferents recorded during normal locomotion in cats. *J Physiol* 507 ( Pt 2): 293-304, 1998a.
- Prochazka A, and Gorassini M.** Models of ensemble firing of muscle spindle afferents recorded during normal locomotion in cats. *J Physiol* 507 ( Pt 1): 277-291, 1998b.
- Proske.** Recent developments in the physiology of the mammalian muscle spindle. In: *Neural control of movement*, edited by Ferrell WR, Proske, U. New York: Plenum Press, 1995.
- Reding MJ, and Potes E.** Rehabilitation outcome following initial unilateral hemispheric stroke. Life table analysis approach. *Stroke* 19: 1354-1358, 1988.
- Ribot-Ciscar E, Bergenheim M, Albert F, and Roll JP.** Proprioceptive population coding of limb position in humans. *Exp Brain Res* 149: 512-519, 2003.
- Sachs O.** The disembodied lady. In: *The man who mistook his wife for a hat and other clinical tales* Summit, 1985.

**Schwartz AB, Kettner RE, and Georgopoulos AP.** Primate motor cortex and free arm movements to visual targets in three-dimensional space. I. Relations between single cell discharge and direction of movement. *J Neurosci* 8: 2913-2927, 1988.

**Scott SH, and Kalaska JF.** Reaching movements with similar hand paths but different arm orientations. I. Activity of individual cells in motor cortex. *J Neurophysiol* 77: 826-852, 1997.

**Scott SH, and Loeb GE.** The computation of position sense from spindles in mono- and multiarticular muscles. *J Neurosci* 14: 7529-7540, 1994.

**Sekhon LH, and Fehlings MG.** Epidemiology, demographics, and pathophysiology of acute spinal cord injury. *Spine* 26: S2-12, 2001.

**Serina ER, Tal R, and Rempel D.** Wrist and forearm postures and motions during typing. *Ergonomics* 42: 938-951, 1999.

**Smetacek V, and Mechsner F.** Making sense. *Nature* 432: 21, 2004.

**Stein R.** *Nerve and muscle membranes, cells, and systems.* New York: Plenum Press, 1980.

**Stein RB, Cody FW, and Capaday C.** The trajectory of human wrist movements. *J Neurophysiol* 59: 1814-1830, 1988.

**Stein RB, Weber DJ, Aoyagi Y, Prochazka A, Wagenaar JB, Shoham S, and Normann RA.** Coding of position by simultaneously recorded sensory neurones in the cat dorsal root ganglion. *J Physiol* 560: 883-896, 2004.

**Sudlow CL, and Warlow CP.** Comparable studies of the incidence of stroke and its pathological types: results from an international collaboration. International Stroke Incidence Collaboration. *Stroke* 28: 491-499, 1997.

**Taylor A, Durbaba R, and Ellaway PH.** Direct and indirect assessment of gamma-motor firing patterns. *Can J Physiol Pharmacol* 82: 793-802, 2004.

**Voss H.** [Tabulation of the absolute and relative muscular spindle numbers in human skeletal musculature]. *Anat Anz* 129: 562-572, 1971.

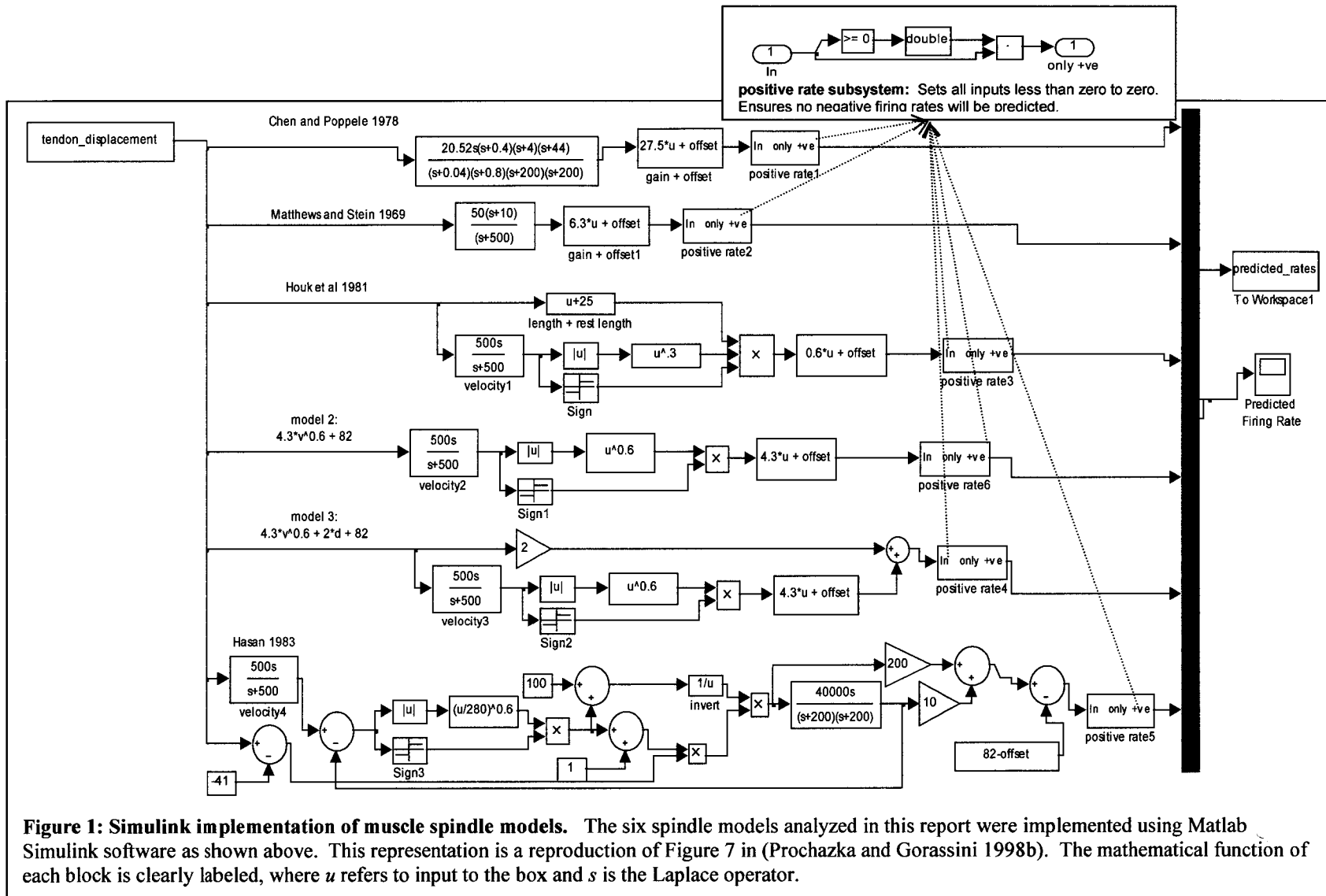
## Appendix - Model Implementations

---

Each of the six spindle models studied in this thesis were previously fit to averaged cat locomotion data (Prochazka and Gorassini 1998b). In order to best meet our main goal of determining whether the same cat spindle models could be generalized to describe human spindles, the same parameters and gains were used as reported in Prochazka & Gorassini. The only adjustment made was in the offset which represents a baseline firing rate of 82 imp/s in the Prochazka & Gorassini implementation and was changed to 10 imp/s in our simulations to better reflect humans. It should be noted that an offset term is not explicit in the Hasan model and thus 72 imp/s was simply subtracted from the original implementations. Alternatively, to reach a baseline firing rate of 10 imp/s in the Hasan model, the parameter  $c$  could be changed from -42 (as fit to the cat data) to -5, but this completely changes the dynamics in the model response and was thus avoided.

The models were implemented using the simulation software Simulink 6.2 in Matlab 7.0.4 with service pack 2 in the same manner as in Figure 7 of (Prochazka and Gorassini 1998b). Since the model files were no longer available on the website cited, models were reproduced from the schematic in Figure 7 of the paper and validated for correct implementation.

Figure 1 shows the Simulink representation of the six models used in this report. Arrows represent the flow of data from one box to the next, where each box represents a processing step such as multiplication, addition, Laplace operation ( $s$  is the Laplace operator), or other pre-defined mathematical functions ( $u$  represents input to a box). The overall input into the Simulink models is muscle stretch in mm, and the overall output is six predicted firing rate series, one series for each model.



In most of the models the muscle velocity is calculated from muscle stretch using the Laplace operation  $500s/(s+500)$ . Only a simple  $s$  operation is necessary to compute a time derivative in the Laplace domain, however the extra  $500/(s+500)$  is used as a low pass filter to smooth out the amplified noise resulting from the derivative process. This is the same filter as used in the Prochazka and Gorassini study. An extra operation was added to the implementation of each model to ensure only positive firing rates were predicted.

Simulations were run with the solver set to handle continuous states using the Euler method with a fixed-step size of 0.001s.

### **Validation**

Before using the implemented models for experimental purposes it was necessary to validate that their realization was correct. For this purpose, cat hamstring muscle length data was manually extracted from Figure 3 in (Prochazka and Gorassini 1998b). The data points were interpolated using the cubic spline method to simulate cat hamstring muscle length trajectory during one step cycle at a sampling rate of 1 kHz. This simulated muscle length data was fed into the models and their output was used to verify conformity with the output of the model implementations in (Prochazka and Gorassini 1998b). It can be seen in Figure 2 that the general shape of firing rate outputs was the same in both implementations, and the nuances of each model were picked up as well, including the sharp dip in the Hasan model and the overestimation in the Matthews and Stein model just after 0.5 seconds into the step cycle. The likeness between the two realizations serves as a validation that models in this report were correctly implemented.

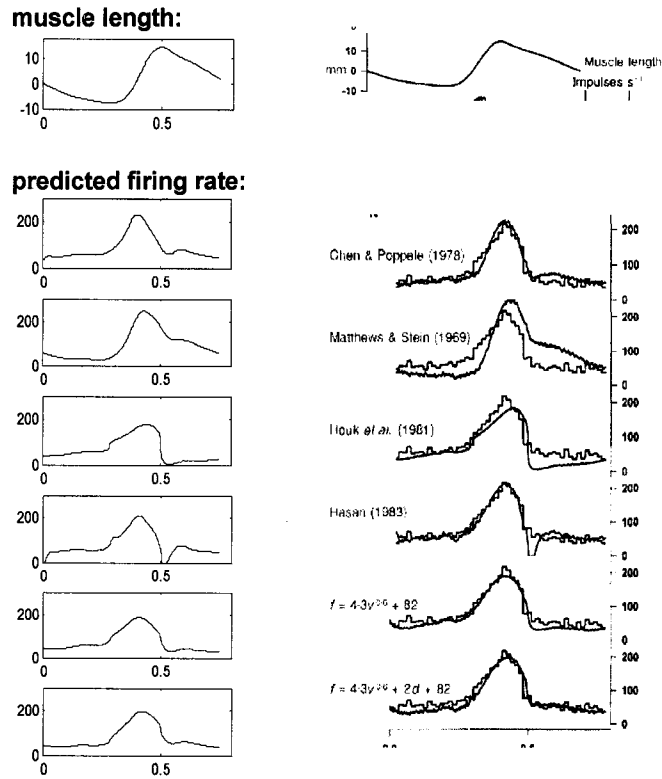


**Figure 2:** Validation of correct model implementation. The predicted firing rates found using six spindle models are shown in response to simulated cat hamstring muscle stretch during one step cycle. On the left is the output of the implementation of models used in this report, with muscle length data extracted from Figure 3 of (Prochazka and Gorassini 1998b) shown on the right. Direct similarities seen in firing rate profiles of figures on the left and right validate that the models were successfully reproduced and correctly implemented in this report.